

Model Reference Adaptive Control Allocation for Constrained Systems with Guaranteed Closed Loop Stability

Seyed Shahabaldin Tohidi ^a, Yildiray Yildiz ^a, Ilya Kolmanovsky ^b

^a*Mechanical Engineering Department, Bilkent University, Ankara, 06800, Turkey*

^b*Department of Aerospace Engineering, University of Michigan, Ann Arbor, MI 48109, USA*

Abstract

This paper proposes an adaptive control allocation approach for uncertain over-actuated systems with actuator saturation. The proposed method does not require uncertainty estimation or a persistent excitation assumption. Using the element-wise non-symmetric projection algorithm, the adaptive parameters are restricted to satisfy certain optimality conditions leading to overall closed loop system stability. Furthermore, a sliding mode controller with a time-varying sliding surface, working in tandem with the adaptive control allocation, is proposed to guarantee the outer loop stability and reference tracking in the presence of control allocation errors and disturbances. Simulation results are provided, where the Aerodata Model in Research Environment is used as an over-actuated system with actuator saturation, to demonstrate the effectiveness of the proposed method.

Key words: Adaptive control; Control allocation; Actuator saturation; Sliding mode control.

Nomenclature

| | |
|----------------------------|--|
| θ_v | Adaptive parameter matrix. |
| θ_{v_j} | The j th column of θ_v . |
| $\theta_{v_{i,j}}$ | The element at the i th row and j th column of θ_v . |
| $\theta_{min_{i,j}}$ | The minimum value of $\theta_{v_{i,j}}$, assigned by the projection algorithm. |
| $\theta_{max_{i,j}}$ | The maximum value of $\theta_{v_{i,j}}$, assigned by the projection algorithm. |
| θ_v^* | Ideal parameter matrix. |
| $\theta_{v_{i,j}}^*$ | The element at the i th row and j th column of θ_v^* . |
| $\theta_{min_{i,j}}^*$ | The minimum value of $\theta_{v_{i,j}}^*$. |
| $\theta_{max_{i,j}}^*$ | The maximum value of $\theta_{v_{i,j}}^*$. |
| θ_I^* | θ_v^* when $\Lambda = I$. |
| $\theta_{I_{i,j}}^*$ | The element at the i th row and j th column of θ_I^* . |
| $\tilde{\theta}_v$ | The deviation of the adaptive parameter matrix from the ideal parameter matrix. |
| $\tilde{\theta}_{v_{i,j}}$ | The element at the i th row and j th column of $\tilde{\theta}_v$. |
| $\tilde{\theta}_{max}$ | The upper bound of the norm of $\tilde{\theta}_v$ when $\theta_{v_{i,j}}^* \in [\theta_{min_{i,j}} \ \theta_{max_{i,j}}]$. |
| $\tilde{\theta}_{MAX}$ | The upper bound of the norm of $\tilde{\theta}_v$ when $\theta_{v_{i,j}}^* \notin [\theta_{min_{i,j}} \ \theta_{max_{i,j}}]$. |

| | |
|----------------|---|
| $\zeta_{i,j}$ | The projection tolerance of the element at the i th row and j th column of θ_v . |
| M_i | The bound on the i th virtual control signal v_i . |
| ρ | The vector of upper bound of the the elements of the disturbance vector d , denoted as $\rho = [\rho_1, \dots, \rho_r]^T$. |
| $\bar{\rho}_i$ | The upper bound of the norm of the i th row of the multiplicative uncertainty (ΔB) . |

1 Introduction

Control allocation is the process of distributing control signals among redundant actuators. Thanks to the benefits of actuator redundancy in systems, such as improved maneuverability, flexibility and fault tolerability, in addition to the decrease in actuator costs due to advances in microprocessors and actuator miniaturization, the number of applications of control allocation has been growing in recent years in such domains as aircraft, spacecraft, unmanned air vehicles [1, 4, 16, 30, 34–36, 47, 49, 50], ships, underwater vehicles [10, 11, 23, 27, 32, 37], automobiles [15, 43], robots [41], and power systems [6, 33].

Control allocation methods can generally be categorized into the following three sets: Pseudo-inverse-based methods, optimization based methods and dynamic control

Email addresses: shahabaldin@bilkent.edu.tr (Seyed Shahabaldin Tohidi), yyildiz@bilkent.edu.tr (Yildiray Yildiz), ilya@umich.edu (Ilya Kolmanovsky).

allocation. Given a mapping between a virtual control input v and the actuator input vector u defined as $Bu = v$, in pseudo inverse based control allocation [2, 17, 18, 44], the control input is distributed to the individual actuators by the pseudo inverse of this mapping $u = B^+v$. It is known that this distribution minimizes the 2-norm of the actuator input vector. This approach can be extended to account for actuator saturation [17, 18, 28, 44]. Daisy chaining [7] and redistributed pseudo inverse [5, 39, 48] are the other modified versions of pseudo inverse method that consider actuator constraints. In optimization based control allocation [8, 24, 25, 31, 51, 52], control input is distributed by minimizing the cost function $|Bu-v| + J_0$, where J_0 refers to secondary objectives such as minimizing actuator deflections. In dynamic control allocation [20, 21, 42, 45, 46, 53], the control signals are distributed among actuators using a set of rules dictated by differential equations. A survey on control allocation methods can be found in [26].

Control allocation is an appealing approach for the design of active fault-tolerant control systems [16, 19, 38, 54]. Optimization based control allocation is used in [43] to improve the performance of steering in faulty automotive vehicles. In another study [32], thruster forces of an autonomous underwater vehicle are allocated among redundant thrusters using control allocation so that faults are accommodated. In [34], experimental results are reported demonstrating the redistribution of the control effort, after a fault, among the redundant actuators of a quadrotor helicopter. In several applications, fault detection and isolation methods are employed in parallel with control allocation [16]. In others, faults are assumed to be estimated a priori. In [2], a sliding mode controller is coupled with a pseudo inverse based control allocation to obtain a fault tolerant controller wherein faults are assumed to be estimated. Similarly in [38], it is assumed that there exists a fault detection and isolation scheme which is able to estimate and identify stuck-in-place, hard-over, loss of effectiveness and floating actuator faults. In [13], an unknown input observer is applied to identify actuator and effector faults. A fault detection and isolation method, for nonlinear systems with redundant actuators, by using a family of unknown input observers is proposed in [14]. In [44] and [8], faults are estimated adaptively using a recursive least square method, and an online dither generation method is proposed to guarantee the persistence of excitation.

This paper proposes an adaptive control allocation method for uncertain systems with redundant actuators in presence of actuator saturation. The method builds upon successful approaches mentioned above by eliminating the need for uncertainty estimation, and therefore it does not require persistence of excitation. Furthermore, in the proposed approach, a closed loop reference model [22] is employed for fast convergence without inducing undesired oscillations. The stability of the overall closed loop system, including the controller,

control allocator and the plant is rigorously studied. Preliminary results of this study were previously presented in [45] and [46]. A modified version of the adaptive control allocation method based on reducing the difference between the derivative of virtual and actual control signals was introduced in [47]. It was demonstrated in [47] that the proposed approach can mitigate pilot induced oscillations. In this paper, we provide the complete picture with an overall closed loop stability proof in the presence of actuator saturation, which was missing in these earlier studies.

Other adaptive approaches to control allocation have been described in [42] and [20]. Different from these approaches, we explicitly consider the actuator saturation, where we guarantee that the control signals remain within their limits all the time, which allows a systematic design of the outer loop controller without assuming its existence a priori.

Apart from the contributions to the control allocation literature mentioned above, we also showed that it is possible to employ the projection algorithm [29] in a stable manner even if the ideal adaptive parameters are not inside the projection boundaries. To the best of our knowledge, this result was not reported earlier in the literature.

This paper is organized as follows. Section II introduces notations and preliminary results. Section III presents the uncertain over-actuated plant dynamics and the proposed model reference adaptive control allocation approach with a closed loop reference model. A discussion of actuator saturation and its effects on virtual control limits together with the projection algorithm are given in Section IV. The controller design, producing the virtual control input, is presented in section V. The ADMIRE model is used in Section VI to demonstrate the effectiveness of the proposed approach in the simulation environment. Finally, a summary is given in Section VII.

2 Background

In this section, we collect several definitions and basic results which are exploited in the following sections. Throughout this paper, $\|\cdot\|$ refers to the Euclidean norm for vectors and induced 2-norm for matrices, and $\|\cdot\|_F$ refers to the Frobenius norm.

The projection operator, denoted as Proj, for two vectors θ and y is defined as [29]

$$\text{Proj}(\theta, y) \equiv \begin{cases} y - \frac{\nabla f(\theta)(\nabla f(\theta))^T}{\|\nabla f(\theta)\|^2} y f(\theta) & \text{if } f(\theta) > 0 \\ & \& y^T \nabla f(\theta) > 0 \\ y & \text{otherwise,} \end{cases} \quad (1)$$

where $f(\cdot)$ is a convex and smooth (C^1) function, and $\nabla(\cdot) : \mathbb{R} \rightarrow \mathbb{R}$ is the gradient operator. If $\theta_v \in \mathbb{R}^{r \times m}$ and $Y \in \mathbb{R}^{r \times m}$ are matrices, the projection operator is defined as

$$\text{Proj}(\theta_v, Y) = (\text{Proj}(\theta_{v,1}, Y_1), \dots, \text{Proj}(\theta_{v,m}, Y_m)), \quad (2)$$

where $\theta_{v,j}$ and Y_j are the j th columns of θ_v and Y , respectively, and $\text{Proj}(\theta_{v,j}, Y_j)$ is defined using (1). A particular choice of (1) is given by

$$\text{Proj}(\theta_{v,j}, Y_j) = (\text{Proj}(\theta_{v_{1,j}}, Y_{1,j}), \dots, \text{Proj}(\theta_{v_{m,j}}, Y_{m,j})), \quad (3)$$

where $\theta_{v_{i,j}}$ and $Y_{i,j}$ are the i th components of $\theta_{v,j}$ and Y_j respectively, and $\text{Proj}(\theta_{v_{i,j}}, Y_{i,j}) : \mathbb{R} \times \mathbb{R} \rightarrow \mathbb{R}$ is an ‘‘element-wise projection’’ defined as

$$\text{Proj}(\theta_{v_{i,j}}, Y_{i,j}) \equiv \begin{cases} Y_{i,j} - Y_{i,j} f(\theta_{v_{i,j}}) & \text{if } f(\theta_{v_{i,j}}) > 0 \\ & \& Y_{i,j} \left(\frac{df(\theta_{v_{i,j}})}{d\theta_{v_{i,j}}} \right) > 0 \\ Y_{i,j} & \text{otherwise,} \end{cases} \quad (4)$$

where $f(\cdot) : \mathbb{R} \rightarrow \mathbb{R}$ is a convex function defined as

$$f(\theta_{v_{i,j}}) = \frac{(\theta_{v_{i,j}} - \theta_{\min_{i,j}} - \zeta_{i,j})(\theta_{v_{i,j}} - \theta_{\max_{i,j}} + \zeta_{i,j})}{(\theta_{\max_{i,j}} - \theta_{\min_{i,j}} - \zeta_{i,j})\zeta_{i,j}}, \quad (5)$$

where $\zeta_{i,j}$ is the projection tolerance of the i, j th element of θ_v that should be chosen as $0 < \zeta_{i,j} < 0.5(\theta_{\max_{i,j}} - \theta_{\min_{i,j}})$. Also, $\theta_{\max_{i,j}}$ and $\theta_{\min_{i,j}}$ are the upper and lower bound of the i, j th element of θ_v . These bounds also form the projection boundary (see figure 1). In comparison to the projection algorithm in [29], the projection algorithm (4) is element-wise and the proposed convex function in (5) considers the cases where $\theta_{\min_{i,j}} \neq -\theta_{\max_{i,j}}$. In the convex function (5), $f(\theta_{v_{i,j}}) = 0$ when $\theta_{v_{i,j}} = \theta_{\max_{i,j}} - \zeta_{i,j}$ or $\theta_{v_{i,j}} = \theta_{\min_{i,j}} + \zeta_{i,j}$, and $f(\theta_{v_{i,j}}) = 1$ when $\theta_{v_{i,j}} = \theta_{\max_{i,j}}$ or $\theta_{v_{i,j}} = \theta_{\min_{i,j}}$.

Lemma 1. If $\dot{\theta}_{v_{i,j}} = \text{Proj}(\theta_{v_{i,j}}, Y_{i,j})$ with initial conditions $\theta_{v_{i,j}}(0) \in \Omega_{i,j} = \{\theta_{v_{i,j}} \in \mathbb{R} | f(\theta_{v_{i,j}}) \leq 1\}$, where $f(\theta_{v_{i,j}}) : \mathbb{R} \rightarrow \mathbb{R}$ is a convex function, then $\theta_{v_{i,j}} \in \Omega_{i,j}$ for $\forall t \geq 0$.

Proof. The proof of Lemma 1. can be found in [22]. \square

Lemma 2. For $\theta_{v_{i,j}}^* \in [\theta_{\min_{i,j}} + \zeta_{i,j}, \theta_{\max_{i,j}} - \zeta_{i,j}]$, $\theta_{v_{i,j}} \in \mathbb{R}^{r \times m}$, $Y \in \mathbb{R}^{r \times m}$ and the projection algorithm in (4) and (5), the following inequality holds:

$$\text{tr} \left((\theta_v^T - \theta_v^{*T})(-Y + \text{Proj}(\theta_v, Y)) \right) \leq 0, \quad (6)$$

where $\text{tr}(\cdot)$ refers to the trace of a matrix.

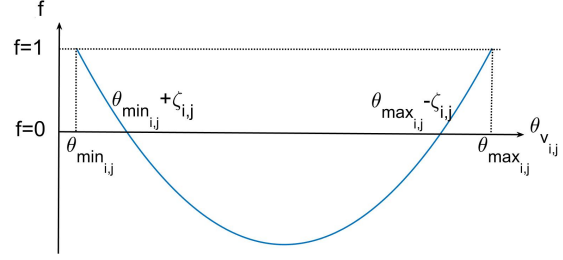


Fig. 1. Convex function $f(\theta_{v_{i,j}})$.

Proof. Let $I_{i,j} = 1$ if $f(\theta_{v_{i,j}}) > 0$ and $Y_{i,j} \left(\frac{df(\theta_{v_{i,j}})}{d\theta_{v_{i,j}}} \right) > 0$, and let $I_{i,j} = 0$, otherwise. Then,

$$\begin{aligned} & \text{tr} \left((\theta_v^T - \theta_v^{*T})(-Y + \text{Proj}(\theta_v, Y)) \right) \\ &= \sum_{j=1}^m \sum_{i=1}^r (\theta_{v_{i,j}} - \theta_{v_{i,j}}^*) (-Y_{i,j} + \text{Proj}(\theta_{v_{i,j}}, Y_{i,j})) \\ &= \sum_{j=1}^m \sum_{i=1}^r (\theta_{v_{i,j}} - \theta_{v_{i,j}}^*) (-Y_{i,j} + Y_{i,j} - Y_{i,j} f(\theta_{v_{i,j}})) I_{i,j} \\ &= \sum_{j=1}^m \sum_{i=1}^r (\theta_{v_{i,j}}^* - \theta_{v_{i,j}}) Y_{i,j} f(\theta_{v_{i,j}}) I_{i,j} \leq 0. \end{aligned}$$

\square

3 Model Reference Adaptive Control Allocation

The closed loop system studied in this paper is presented in Figure 2. Consider the following plant dynamics,

$$\dot{x} = Ax + B_u(\Lambda u + d_u), \quad (7)$$

where $x \in \mathbb{R}^n$ is the state vector, $u = [u_1, \dots, u_m]^T \in \mathbb{R}^m$ is the actuator input vector, where $u_i \in [-u_{\max_i}, u_{\max_i}]$, $A \in \mathbb{R}^{n \times n}$ is the known state matrix, $B_u \in \mathbb{R}^{n \times m}$ is the known input matrix and $d_u \in \mathbb{R}^m$ is a bounded disturbance input. The matrix $\Lambda \in \mathbb{R}^{m \times m}$ is assumed to be diagonal, with non-negative elements representing actuator effectiveness uncertainty. It is assumed that the pair $(A, B_u \Lambda)$ is controllable. Due to actuator redundancy, the input matrix is rank deficient, that is $\text{Rank}(B_u) = r < m$. Consequently, B_u can be written as $B_u = B_v B$, where $B_v \in \mathbb{R}^{n \times r}$ is a full column rank matrix, i.e. $\text{Rank}(B_v) = r$, and $B \in \mathbb{R}^{r \times m}$. The decomposition of B_u helps exploit the actuator redundancy using control allocation. Employing this decomposition, (7) can be rewritten as

$$\dot{x} = Ax + B_v(B \Lambda u + \bar{d}), \quad (8)$$

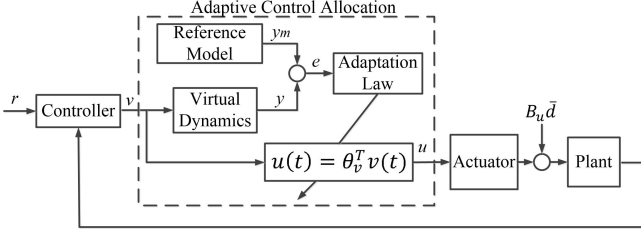


Fig. 2. Block diagram of the closed loop system with the proposed adaptive control allocation method.

where $\bar{d}(t) = B_d u(t)$ is assumed to have an upper bound $\|\bar{d}(t)\| \leq \bar{L}$, for all $t \geq 0$. The control allocation task is to achieve

$$B\Lambda u + \bar{d} = v, \quad (9)$$

where $v \in \mathbb{R}^n$ is the virtual control signal and also the output of the nominal controller which will be defined in Section V (See Figure 2). Considering the following dynamics,

$$\dot{y} = A_m y + B\Lambda u + \bar{d} - v, \quad (10)$$

where $A_m \in \mathbb{R}^{r \times r}$ is a stable (Hurwitz) matrix, a reference model is constructed as

$$\dot{y}_m = A_m y_m. \quad (11)$$

Defining the actuator input as a mapping from v to u ,

$$u = \theta_v^T v, \quad (12)$$

where $\theta_v \in \mathbb{R}^{r \times m}$ represents the adaptive parameter matrix to be determined, and substituting (12) into (10), we obtain

$$\dot{y} = A_m y + (B\Lambda \theta_v^T - I_r)v + \bar{d}, \quad (13)$$

where I_r is an identity matrix of dimension $r \times r$.

It is assumed that there exists an ideal matrix θ_v^* such that

$$B\Lambda \theta_v^{*T} = I_r. \quad (14)$$

Defining $e = y - y_m$ and subtracting (11) from (13), it follows that

$$\dot{e} = A_m e + B\Lambda \tilde{\theta}_v^T v + \bar{d}, \quad (15)$$

where $\tilde{\theta}_v = \theta_v - \theta_v^*$.

Theorem 1. If the adaptive parameter matrix (10) is updated using the following adaptive law,

$$\dot{\theta}_v = \Gamma_\theta \text{Proj}(\theta_v, -ve^T PB), \quad (16)$$

where the projection operator ‘‘Proj’’ is defined in (4), with convex and smooth (C^1) function $f(\theta_{v_{i,j}})$ in (5), and where $\Gamma_\theta = \gamma_\theta I_r$, $\gamma_\theta > 0$, then given any initial

condition $e(0) \in \mathbb{R}^r$, $\theta_{v_{i,j}}(0) \in [\theta_{\min_{i,j}}, \theta_{\max_{i,j}}]$, and $\theta_{v_{i,j}}^* \in [\theta_{\min_{i,j}} + \zeta_{i,j}, \theta_{\max_{i,j}} - \zeta_{i,j}]$, $e(t)$ and $\tilde{\theta}_v(t)$ remain uniformly bounded for all $t \geq 0$ and their trajectories converge exponentially to the set

$$E_1 = \{(e, \tilde{\theta}_v) : \|e\|^2 \leq \left(\frac{s\tilde{\theta}_{\max}^2}{\gamma_\theta} + \frac{2m^4\bar{L}^2}{\sigma^2}\right) \frac{4sm^2}{\sigma}, \quad (17)$$

$$\|\tilde{\theta}_v\| \leq \tilde{\theta}_{\max}\},$$

where constants s , σ , m and $\tilde{\theta}_{\max}$ will be defined in the proof of the theorem.

Proof. Consider a Lyapunov function candidate,

$$V = e^T P e + \text{tr}(\tilde{\theta}_v^T \Gamma_\theta^{-1} \tilde{\theta}_v \Lambda), \quad (18)$$

where $\Gamma_\theta = \Gamma_\theta^T = \gamma_\theta I_r$, $\gamma_\theta > 0$, tr refers to the trace operation and P is the positive definite symmetric matrix solution of the Lyapunov equation,

$$A_m^T P + P A_m = -Q, \quad (19)$$

and where Q is a symmetric positive definite matrix. The derivative of the Lyapunov function candidate (18) along the trajectories of (15)-(16) can be calculated as

$$\begin{aligned} \dot{V} &= e^T (A_m P + P A_m) e + 2e^T P B \Lambda \tilde{\theta}_v^T v \\ &\quad + 2\text{tr}(\tilde{\theta}_v^T \Gamma_\theta^{-1} \dot{\tilde{\theta}}_v \Lambda) + 2e^T P \bar{d} \\ &= -e^T Q e + 2e^T P B \Lambda \tilde{\theta}_v^T v + 2\text{tr}(\tilde{\theta}_v^T \Gamma_\theta^{-1} \dot{\tilde{\theta}}_v \Lambda) + 2e^T P \bar{d}. \end{aligned} \quad (20)$$

Using the property of the trace operation, $a^T b = \text{tr}(ba^T)$ where a and b are vectors, (20) can be rewritten as

$$\dot{V} = -e^T Q e + 2\text{tr}\left(\tilde{\theta}_v^T \left(ve^T PB + \Gamma_\theta^{-1} \dot{\tilde{\theta}}_v\right) \Lambda\right) + 2e^T P \bar{d}. \quad (21)$$

Using the following adaptive law,

$$\dot{\theta}_v = \Gamma_\theta \text{Proj}(\theta_v, -ve^T PB), \quad (22)$$

(21) can be written as

$$\begin{aligned} \dot{V} &= -e^T Q e + 2e^T P \bar{d} \\ &\quad + 2\text{tr}\left(\tilde{\theta}_v^T \left(ve^T PB + \text{Proj}(\theta_v, -ve^T PB)\right) \Lambda\right). \end{aligned} \quad (23)$$

In the absence of a disturbance \bar{d} , it can be shown, by using Lemma 2, that $\dot{V} \leq 0$ and therefore e and $\tilde{\theta}_v$ are bounded. Furthermore, using Barbalat’s lemma it can be shown that the error e converges to zero. When $\bar{d} \neq 0$, it can be shown that all the trajectories converge to a

compact set E_1 . To find E_1 , it is necessary to define the following parameters [22]

$$\sigma \equiv -\max_i(\text{Real}(\lambda_i(A_m))), \quad (24)$$

$$s \equiv -\min_i(\lambda_i(A_m + A_m^T)/2), \quad (25)$$

$$a \equiv \|A_m\|, \quad (26)$$

where $\lambda_i(A_m)$ refers to the i th eigenvalue of the matrix A_m . If the matrix Q in (19) is selected as an identity matrix of dimension $r \times r$, then the matrix P satisfies the following properties [22]

$$\|P\| \leq \frac{m^2}{\sigma}, \quad (27)$$

$$\lambda_{\min}(P) \geq \frac{1}{2s}, \quad (28)$$

where σ and s are defined in (24) and (25), $\lambda_{\min}(\cdot)$ denotes the minimum eigenvalue and $m = \frac{3}{2}(1 + 4\frac{a}{\sigma})^{(r-1)}$, and where a is defined in (26).

Using the Lyapunov function candidate (18), it follows that

$$\begin{aligned} V &= e^T P e + \text{tr}(\tilde{\theta}_v^T \Gamma_\theta^{-1} \tilde{\theta}_v \Lambda) \\ &\leq \|e\|^2 \|P\| + \text{tr}(\tilde{\theta}_v^T \Gamma_\theta^{-1} \tilde{\theta}_v \Lambda) \\ &= \|e\|^2 \|P\| + (1/\gamma_\theta) \text{tr}(\tilde{\theta}_v^T \tilde{\theta}_v \Lambda) \\ &\leq \|e\|^2 \|P\| + (1/\gamma_\theta) \|\tilde{\theta}_v\|_F^2 \\ &\leq \|e\|^2 \|P\| + (1/\gamma_\theta) \tilde{\theta}_{\max}^2, \end{aligned} \quad (29)$$

where $\Gamma_\theta^{-1} = (1/\gamma_\theta)I_r$, $\gamma_\theta > 0$, $\Lambda = \text{diag}(\lambda_1, \dots, \lambda_m)$, $0 < \lambda_i \leq 1$ and considering $\theta_{v_{i,j}}^* \in [\theta_{\min_{i,j}} + \zeta_{i,j}, \theta_{\max_{i,j}} - \zeta_{i,j}]$ and using (5), we have $\|\tilde{\theta}_v(t)\|_F \leq \tilde{\theta}_{\max}$, for all $t \geq 0$, where $\tilde{\theta}_{\max}$ is defined as

$$\tilde{\theta}_{\max} \equiv \sqrt{\sum_{i,j} (\theta_{\max_{i,j}} - \theta_{\min_{i,j}} - \zeta_{i,j})^2}. \quad (30)$$

Using (29), we have

$$\frac{V}{\|P\|} - \frac{\tilde{\theta}_{\max}^2}{\gamma_\theta \|P\|} \leq \|e\|^2. \quad (31)$$

Since $\theta_{v_{i,j}}^* \in [\theta_{\min_{i,j}} + \zeta_{i,j}, \theta_{\max_{i,j}} - \zeta_{i,j}]$, using (23), (6), and considering $Q = I_r$, we have $\dot{V} \leq -\|e\|^2 + 2\|e\|\|P\bar{d}\|$. In addition, by using the inequality,

$$|xy| \leq \frac{x^2}{2c} + \frac{c|y|^2}{2}, \quad (32)$$

for $c = 2$, $x = \|e\|$, $y = \|P\bar{d}\|$, it follows that we have $2\|e\|\|P\bar{d}\| \leq \frac{1}{2}\|e\|^2 + 2\|P\bar{d}\|^2$. Recalling that the upper bound of \bar{d} is \bar{L} , it follows that $\dot{V} \leq -\frac{1}{2}\|e\|^2 + 2\|P\|^2 \bar{L}^2$. Thus, using (31), we have

$$\begin{aligned} \dot{V}(t) &\leq -\frac{1}{2}\|e\|^2 + 2\|P\|^2 \bar{L}^2 \\ &\leq -\frac{V}{2\|P\|} + \frac{\tilde{\theta}_{\max}^2}{2\gamma_\theta \|P\|} + 2\|P\|^2 \bar{L}^2 \leq -\omega_1 V + \omega_2, \end{aligned} \quad (33)$$

where $\omega_1 = \frac{\sigma}{2m^2}$ and $\omega_2 = \frac{s}{\gamma_\theta} \tilde{\theta}_{\max}^2 + \frac{2m^4 \bar{L}^2}{\sigma^2}$. By using the Gronwall inequality, whose statement is that for $\dot{V}(t) \leq b(t)V(t) + h(t)$, we have

$$V(t) \leq V(0) \exp\left(\int_\alpha^t b(s) ds\right) + \int_\alpha^t h(s) \exp\left(\int_s^t b(\tau) d\tau\right) ds, \quad (34)$$

(33) can be rewritten as

$$V(t) \leq \left(V(0) - \frac{\omega_2}{\omega_1}\right) e^{-\omega_1 t} + \frac{\omega_2}{\omega_1}. \quad (35)$$

Using $e(t)^T P e(t) \leq V(t) \leq \left(V(0) - \frac{\omega_2}{\omega_1}\right) e^{-\omega_1 t} + \frac{\omega_2}{\omega_1}$ and taking the limits of the leftmost and rightmost sides as t goes to infinity, we have

$$\limsup_{t \rightarrow \infty} e(t)^T P e(t) \leq \frac{\omega_2}{\omega_1} = \left(\frac{s\tilde{\theta}_{\max}^2}{\gamma_\theta} + \frac{2m^4 \bar{L}^2}{\sigma^2}\right) \frac{2m^2}{\sigma}. \quad (36)$$

By using the following inequality

$$\lambda_{\min}(P) \|e\|^2 \leq e^T P e \leq \lambda_{\max}(P) \|e\|^2, \quad (37)$$

and (28), we have

$$\frac{1}{2s} \|e\|^2 \leq \lambda_{\min}(P) \|e\|^2 \leq e^T P e. \quad (38)$$

By using (36) and taking the limit of both sides of (38) as t goes to infinity,

$$\limsup_{t \rightarrow \infty} \|e(t)\|^2 \leq \left(\frac{s\tilde{\theta}_{\max}^2}{\gamma_\theta} + \frac{2m^4 \bar{L}^2}{\sigma^2}\right) \frac{4sm^2}{\sigma}. \quad (39)$$

Therefore, for the initial conditions $e(0)$ and $\theta_{v_{i,j}}(0) \in [\theta_{\min_{i,j}} + \zeta_{i,j}, \theta_{\max_{i,j}} - \zeta_{i,j}]$, $e(t)$ and $\tilde{\theta}_v(t)$ are uniformly bounded for all $t \geq 0$ and system trajectories converge to the following compact set

$$E_1 = \{(e, \tilde{\theta}_v) : \|e\|^2 \leq \left(\frac{s\tilde{\theta}_{\max}^2}{\gamma_\theta} + \frac{2m^4 \bar{L}^2}{\sigma^2}\right) \frac{4sm^2}{\sigma}, \|\tilde{\theta}_v\| \leq \tilde{\theta}_{\max}\}. \quad (40)$$

□

It is noted that the bound on $\tilde{\theta}_v$ in (40) is a direct result of Lemma 1 and the definition given in (30).

The analysis provided above shows that θ_v and e are bounded. Assuming that v is bounded, (12) implies that u is bounded. In the sequel, the boundedness of v will be established by using a soft saturation bound on v during the design of the controller, the effect of which will be analyzed in section 5.3. Since A_m is Hurwitz, the variable y , whose dynamics is given in (10), is also bounded. Therefore, all the signals in the adaptive control allocation system are bounded.

Remark 1. Note that $\theta_v^* \in \mathbb{R}^{r \times m}$ is the ideal parameter matrix that should satisfy (14). Since Λ is unknown, θ_v^* is also unknown. However, although the diagonal matrix Λ is unknown, the range of its elements can be taken as $(0, 1]$, assuming that the uncertainty originates from possible loss of actuator effectiveness. Thus, using (14), the range of θ_v^* can be obtained, and expressed as $\theta_{i,j}^* \in [\theta_{min_{i,j}}^*, \theta_{max_{i,j}}^*]$.

Remark 2. Let $[\theta_{min_{i,j}}, \theta_{max_{i,j}}] \subset [\theta_{min_{i,j}}^*, \theta_{max_{i,j}}^*]$ and $\theta_{v_{i,j}}^* \notin [\theta_{min_{i,j}} + \zeta_{i,j}, \theta_{max_{i,j}} - \zeta_{i,j}]$, and consider the projection algorithm (4) with convex function (5). Then, $\tilde{\theta}_{max}$, which was defined in (30), should be redefined so that $\|\tilde{\theta}_v(t)\|_F \leq \tilde{\theta}_{MAX}$, for all $t \geq 0$, where $\tilde{\theta}_{MAX}$ is defined as

$$\tilde{\theta}_{MAX} \equiv \sqrt{\sum_{i,j} (\max(|\theta_{max_{i,j}}^* - \theta_{min_{i,j}}|, |\theta_{min_{i,j}}^* - \theta_{max_{i,j}}|))^2}. \quad (41)$$

We note that to delineate two different cases (the ideal parameter θ_v^* being inside or outside the projection bounds), the maximum value of adaptive parameter deviation from its ideal value is designated by $\tilde{\theta}_{max}$ for the former and $\tilde{\theta}_{MAX}$ for the latter case. Below, we provide a lemma and a theorem, regarding the stability of the control allocation for the latter case, i.e. when $\theta_{v_{i,j}}^* \notin [\theta_{min_{i,j}} + \zeta_{i,j}, \theta_{max_{i,j}} - \zeta_{i,j}]$.

Lemma 3. For $\theta_{v_{i,j}}^* \notin [\theta_{min_{i,j}} + \zeta_{i,j}, \theta_{max_{i,j}} - \zeta_{i,j}]$, $\theta_{v_{i,j}} \in \mathbb{R}^{r \times m}$, $Y \in \mathbb{R}^{r \times m}$ with $r \leq m$ and the projection algorithm (4)-(5), the following inequality holds:

$$\text{tr} \left((\theta_v^T - \theta_v^{*T})(-Y + \text{Proj}(\theta_v, Y)) \right) \leq \sqrt{r} \tilde{\theta}_{MAX} \|Y\|. \quad (42)$$

Proof. For both cases in projection algorithm (4), we

have

$$\begin{aligned} & \text{tr} \left((\theta_v^T - \theta_v^{*T})(-Y + \text{Proj}(\theta_v, Y)) \right) \\ &= \sum_{j=1}^m \sum_{i=1}^r (\theta_{v_{i,j}} - \theta_{v_{i,j}}^*) (-Y_{i,j} + \text{Proj}(\theta_{v_{i,j}}, Y_{i,j})) \\ &\leq \sum_{j=1}^m \sum_{i=1}^r |(\theta_{v_{i,j}} - \theta_{v_{i,j}}^*) Y_{i,j} f(\theta_{v_{i,j}})| \\ &\leq \sum_{j=1}^m \sum_{i=1}^r |\tilde{\theta}_{i,j} Y_{i,j}| = \text{tr}(|\tilde{\theta}_v^T| |Y|) \\ &\leq \|\tilde{\theta}_v\|_F \|Y\|_F \leq \sqrt{r} \|\tilde{\theta}_v\|_F \|Y\| \leq \sqrt{r} \tilde{\theta}_{MAX} \|Y\|, \end{aligned}$$

where we used the property, $\|Y\|_F \leq \sqrt{\min(r, m)} \|Y\|$, and $|\tilde{\theta}_v^T|$ and $|Y|$ which are the matrices of absolute values of the elements of $\tilde{\theta}_v^T$ and Y , respectively. □

Theorem 2. Consider (10), the reference model (11), the controller (12), and the adaptive law,

$$\dot{\theta}_v = \Gamma_\theta \text{Proj}(\theta_v, -ve^T P B), \quad (43)$$

where $\Gamma_\theta^{-1} = (1/\gamma_\theta) I_r$, $\gamma_\theta > 0$, and the projection is defined in (4) and (5). Assume $\|v(t)\| \leq M$ and $\|\bar{d}(t)\| \leq \bar{L}$ for all $t \geq 0$. Then, for any initial condition $e(0) \in \mathbb{R}^r$, $\theta_{v_{i,j}}(0) \in [\theta_{min_{i,j}}, \theta_{max_{i,j}}]$, and $\theta_{v_{i,j}}^* \notin [\theta_{min_{i,j}} + \zeta_{i,j}, \theta_{max_{i,j}} - \zeta_{i,j}]$, $e(t)$ and $\tilde{\theta}_v(t)$ are uniformly bounded for all $t \geq 0$ and their trajectories converge exponentially to

$$\begin{aligned} \hat{E}_1 = \{ (e, \tilde{\theta}_v) : & \|\tilde{\theta}_v\| \leq \tilde{\theta}_{MAX}, \|e\|^2 \leq \left(\frac{s \tilde{\theta}_{MAX}^2}{\gamma_\theta} \right. \\ & \left. + \frac{4m^4 \bar{L}^2 + 4r \tilde{\theta}_{MAX}^2 m^4 \|B\|^2 M^2}{\sigma^2} \right) \frac{4sm^2}{\sigma} \}, \quad (44) \end{aligned}$$

where the constants σ , s and m are defined in the proof of Theorem 1 and $\tilde{\theta}_{MAX}$ is defined in Remark 2.

Proof. By using (18), (19) with $Q = I_r$, (23) and (42) with $Y = -ve^T P B$, we have

$$\begin{aligned} \dot{V} &\leq -\|e\|^2 + 2\|e\| \|P\| \bar{L} + 2\sqrt{r} \tilde{\theta}_{MAX} \|Y\| \\ &\leq -\|e\|^2 + 2\|e\| \|P\| \bar{L} + 2\sqrt{r} \tilde{\theta}_{MAX} \|e\| \|P\| \|B\| M, \quad (45) \end{aligned}$$

where $\|\bar{d}\| \leq \bar{L}$ and v is the control command vector produced by the controller with an upper bound M .

By using the inequality (32) with $x = \|e\|$, $y = 2\|P\| \bar{L}$, $c = 2$ for $2\|e\| \|P\| \bar{L}$ in (45), and $x = \|e\|$, $y = 2\sqrt{r} \tilde{\theta}_{MAX} \|P\| \|B\| M$, $c = 2$ for $2\sqrt{r} \tilde{\theta}_{MAX} \|e\| \|P\| \|B\| M$

in (45), we obtain that

$$\dot{V} \leq -\frac{1}{2}\|e\|^2 + 4\|P\|^2\bar{L}^2 + 4r\tilde{\theta}_{MAX}^2\|P\|^2\|B\|^2M^2. \quad (46)$$

Using (31), we obtain that

$$\begin{aligned} \dot{V} &\leq -\frac{V}{2\|P\|} + \frac{\tilde{\theta}_{MAX}^2}{2\gamma_\theta\|P\|} + 4\|P\|^2\bar{L}^2 \\ &+ 4r\tilde{\theta}_{MAX}^2\|P\|^2\|B\|^2M^2 \leq -\hat{\omega}_1V + \hat{\omega}_2, \end{aligned} \quad (47)$$

where $\hat{\omega}_1 = \frac{\sigma}{2m^2}$ and $\hat{\omega}_2 = \frac{s}{\gamma_\theta}\tilde{\theta}_{MAX}^2 + 4\frac{m^4\bar{L}^2}{\sigma^2} + 4\frac{r\tilde{\theta}_{MAX}^2m^4\|B\|^2M^2}{\sigma^2}$, and where σ and s are defined in (24) and (25). Following the same procedure as for E_1 , \hat{E}_1 is obtained as

$$\begin{aligned} \hat{E}_1 &= \{(e, \tilde{\theta}_v) : \|\tilde{\theta}_v\| \leq \tilde{\theta}_{MAX}, \|e\|^2 \leq (\frac{s\tilde{\theta}_{MAX}^2}{\gamma_\theta} \\ &+ \frac{4m^4\bar{L}^2 + 4r\tilde{\theta}_{MAX}^2m^4\|B\|^2M^2}{\sigma^2})\frac{4sm^2}{\sigma}\}. \end{aligned} \quad (48)$$

□

Remark 3. A discussion about putting an upper bound M on the control command, without assuming a stable control allocation, is given in section IV.

To obtain fast convergence without introducing excessive oscillations, the open loop reference model (11) is modified to obtain the following closed loop reference model [22].

$$\dot{y}_m = A_m y_m - L(y - y_m), \quad (49)$$

where $A_m \in \mathbb{R}^{r \times r}$ is Hurwitz, $L = -\ell I_r$, $\ell > 0$, and $I_r \in \mathbb{R}^{r \times r}$ is an identity matrix. Defining $\bar{A}_m = A_m + L$, and subtracting (49) from (13), it follows that

$$\dot{e} = \bar{A}_m e + B\Lambda\tilde{\theta}_v^T v + \bar{d}. \quad (50)$$

We assume that the matrix \bar{A}_m is made Hurwitz through an appropriate selection of L .

Theorem 3. Consider (10), the reference model (49), the controller (12), and the adaptive law

$$\dot{\theta}_v = \Gamma_\theta \text{Proj}(\theta_v, -ve^T P B), \quad (51)$$

where $\Gamma_\theta^{-1} = (1/\gamma_\theta)I_r$, $\gamma_\theta > 0$ and the projection is defined by (4) and (5). For any initial condition $e(0) \in \mathbb{R}^r$,

and $\theta_{v_{i,j}}(0) \in [\theta_{min_{i,j}}, \theta_{max_{i,j}}]$, $e(t)$ and $\tilde{\theta}(t)$ are uniformly bounded for all $t \geq 0$ and their trajectories converge exponentially to a closed and bounded set defined either by (60) or (61) in the proof of Theorem 3.

Proof. Consider the following Lyapunov function candidate,

$$V_1 = e^T \bar{P} e + tr(\tilde{\theta}_v^T \Gamma_\theta^{-1} \tilde{\theta}_v \Lambda), \quad (52)$$

where \bar{P} is the symmetric positive definite matrix solution of the following Lyapunov equation,

$$\bar{A}_m^T \bar{P} + \bar{P} \bar{A}_m = -I_r, \quad (53)$$

where I_r is an identity matrix of dimension $r \times r$. The time derivative of V_1 along the trajectories of (50)-(51) can be obtained as

$$\dot{V}_1 = -e^T \bar{Q} e + 2e^T P \bar{d} + 2tr\left(\tilde{\theta}_v^T (ve^T \bar{P} B + \Gamma_\theta^{-1} \dot{\tilde{\theta}}_v) \Lambda\right). \quad (54)$$

Assume first that $\theta_{v_{i,j}}^* \in [\theta_{min_{i,j}} + \zeta_{i,j}, \theta_{max_{i,j}} - \zeta_{i,j}]$.

To find the set to which e and $\tilde{\theta}_v$ converge, it is necessary to define the following parameters [22]

$$\bar{\sigma} \equiv -\max_i(\text{Real}(\lambda_i(\bar{A}_m))), \quad (55)$$

$$\bar{s} \equiv -\min_i(\lambda_i(\bar{A}_m + \bar{A}_m^T)/2), \quad (56)$$

$$\bar{a} \equiv \|\bar{A}_m\|. \quad (57)$$

Then, \bar{P} satisfies the following properties [22]:

$$\|\bar{P}\| \leq \frac{\bar{m}^2}{\bar{\sigma} + 2\ell}, \quad (58)$$

$$\lambda_{\min}(\bar{P}) \geq \frac{1}{2(\bar{s} + \ell)}, \quad (59)$$

where $\lambda_{\min}(\cdot)$ denotes the minimum eigenvalue and $\bar{m} = \frac{3}{2}(1 + 4\frac{\bar{a}}{\bar{\sigma}})^{(r-1)}$.

Proceeding as in the proof of Theorem 1, and using (55-57), for the initial conditions $e(0)$ and $\|\tilde{\theta}_v(0)\| \leq \tilde{\theta}_{max}$, e and $\tilde{\theta}_v$ can be shown to be uniformly bounded and converge to the following set,

$$\begin{aligned} E_2 &= \{(e, \tilde{\theta}_v) : \|e\|^2 \leq (\frac{(\bar{s} + \ell)\tilde{\theta}_{max}^2}{\gamma_\theta} + \frac{2\bar{m}^4\bar{L}^2}{(\bar{\sigma} + 2\ell)^2}) \\ &\times \frac{4(\bar{s} + \ell)\bar{m}^2}{(\bar{\sigma} + 2\ell)}, \|\tilde{\theta}_v\| \leq \tilde{\theta}_{max}\}. \end{aligned} \quad (60)$$

If $\theta_{v_{i,j}}^* \notin [\theta_{min_{i,j}} + \zeta_{i,j}, \theta_{max_{i,j}} - \zeta_{i,j}]$, proceeding similar as in the proof of Theorem 2, the convergence set is

characterized as

$$\begin{aligned} \hat{E}_2 = \{ (e, \tilde{\theta}_v) : \|e\|^2 \leq & \left(\frac{(\bar{s} + \ell)\tilde{\theta}_{MAX}^2}{\gamma_\theta} + \frac{4\bar{m}^4\bar{L}^2}{(\bar{\sigma} + 2\ell)^2} \right. \\ & \left. + \frac{4r\tilde{\theta}_{MAX}^2\bar{m}^4\|B\|^2M^2}{(\bar{\sigma} + 2\ell)^2} \right) \frac{4(\bar{s} + \ell)\bar{m}^2}{(\bar{\sigma} + 2\ell)}, \\ \|\tilde{\theta}_v\| \leq & \tilde{\theta}_{MAX} \}. \end{aligned} \quad (61)$$

□

4 Determination of the projection boundaries

In the previous section, the adaptive control allocator was designed based on the projection operator and proved to be stable. In this section, the selection of the projection boundaries, which define the bounds on adaptive control parameters, is explained. The projection boundaries are determined to satisfy two requirements: 1) The actuator command signals should not saturate the actuators and 2) a specific requirement in the controller design, which will be provided in the following subsections, to obtain a stable closed loop system, including the controller, the control allocator and the plant (see Fig. 2), should be satisfied. The design procedure to achieve these goals is composed of three main steps. In the first step, an attainable set for virtual control signal vector v is found in the absence of disturbance based on the actuators constraints and $v = B\Lambda u$. In the second step, using the calculated attainable set for v , projection bounds are calculated to satisfy $-u_{max} \leq \theta_v^T v \leq u_{max}$. In the first two steps, the attainable sets are obtained, and as long as the signals are inside these set, we can guarantee that the actuator constraints are satisfied. In the third step, a subset of the projection boundaries calculated in step 2 that satisfies an overall closed loop stability requirement is determined.

Step 1

In this step, realizable values of virtual control signals are found.

Note that the actuator constraints are known: $u(t) \in \Omega_u$, where $\Omega_u = \{[u_1, \dots, u_m]^T : -u_{max_i} \leq u_i \leq u_{max_i}, i = 1, \dots, m\}$. Therefore, using Ω_u , the set $\Omega_v \in \mathbb{R}^r$, defining all realizable values of the virtual control input v , can be obtained as $\Omega_v = \{v : v = Bu, u \in \Omega_u, B^T v \in \Omega_u\}$. Note that Ω_v also defines the upper and lower bounds of each element of the realizable virtual control, $v = [v_1, \dots, v_r]^T$. To make sure that v_i remains within its realizable bounds, $v_i \in [-M_i, M_i], \forall i = 1, \dots, r$, we use a soft saturation bound on the control signal v . In Section V, we will design the controller by taking this saturation bound into account.

Step 2

The projection boundaries that limit the adaptive parameters are calculated in this step, to make sure that the actuator signal vector u does not saturate the actuators.

From Step 1, we obtained the attainable set for the virtual control signals (Ω_v). The actuator limits, u_{max} and $u_{min} = -u_{max}$ are known. With this information, the set $\Omega_\theta = \{vec(\theta_v) : -u_{max} \leq \theta_v^T v \leq u_{max}, v \in \Omega_v\}$, where $vec(\cdot) : \mathbb{R}^{r \times m} \rightarrow \mathbb{R}^{rm}$ puts the elements of a matrix in a column vector, can be obtained. Note that $\theta_I^* \in \Omega_\theta$, that is, in the absence of any uncertainty, the ideal adaptive parameter matrix, θ_I^* , always exists in Ω_θ . This leads to the smallest convergence set for error trajectories when $\Lambda = I$.

Step 3

In this step, a subset of Ω_θ , which satisfies a necessary condition for controller stability, is obtained. This subset of Ω_θ also determines the ultimate projection boundaries, and is denoted by Ω_{proj} .

After Step 2, establishing that the control allocation output, which is the actuator input signal vector u , does not saturate the actuators, the plant dynamics (8) can be rewritten, by using (12), (14) and defining $\tilde{\theta}_v = \theta_v - \theta_v^*$, as

$$\begin{aligned} \dot{x} &= Ax + B_v(B\Lambda u + \bar{d}) \\ &= Ax + B_v(B\Lambda\theta_v^T v + \bar{d}) \\ &= Ax + B_v(I + B\Lambda\tilde{\theta}_v^T)v + B_v\bar{d}. \end{aligned} \quad (62)$$

Defining $\Delta B \equiv B\Lambda\tilde{\theta}_v^T$, and substituting in (62), it follows that

$$\dot{x} = Ax + B_v(v + d), \quad (63)$$

where $d = \Delta Bv + \bar{d} \in \mathbb{R}^r$.

To be able to design a stabilizing controller, one must make sure that the i th element of the disturbance vector $d = [d_1, \dots, d_r]^T$ in (63), is smaller in absolute value than the upper bound of the i th element of the virtual control input which was defined in Step 1, that is $|d_i| < M_i$, $i = 1, \dots, r$. Since each $d_i = \text{row}_i(\Delta B)v + \bar{d}_i$, where \bar{d}_i is the i th element of \bar{d} , and $\text{row}_i(\cdot)$ designates the i th row of a matrix, satisfying the following condition ensures that $|d_i| < M_i$, $i = 1, \dots, r$:

$$M_i - \|\text{row}_i(\Delta B)\|M_{\max} > |\bar{d}_i|, \quad i = 1, \dots, r, \quad (64)$$

where $M_{\max} = \max_i M_i$. A necessary condition for satisfying the inequality (64), is $\|\text{row}_i(\Delta B)\| = \|\text{row}_i(B\Lambda\tilde{\theta}_v^T)\| < \frac{M_i}{M_{\max}}$ for all $i = 1, \dots, r$. (Sufficient conditions required to satisfy (64) will be discussed later in Remark 4). Thus, the elements of the matrix θ_v should be properly bounded in order to satisfy the necessary condition $\|\text{row}_i(B\Lambda\tilde{\theta}_v^T)\| < \frac{M_i}{M_{\max}}$ for all $i = 1, \dots, r$, and for all $\Lambda \in \Omega_{\Lambda_1}$, where $\Omega_{\Lambda_1} \subset \Omega_{\Lambda}$, and Ω_{Λ} is the set of all

$m \times m$ diagonal matrices with elements in $[0, 1]$; furthermore, Ω_{Λ_1} should have diagonal elements $\lambda_i \in (\gamma, 1]$, where γ is precisely defined later in Theorem 4.

Remark 4. In order to find a non-empty set, for which the elements of θ_v satisfy the necessary condition discussed above, an optimization problem needs to be solved over the following set,

$$E = \{\text{vec}(\theta_v) : \|\text{row}_i(B\Lambda\theta_v^T - I_r)\|^2 \leq \frac{M_i^2}{M_{\max}^2} - \epsilon, \Lambda \in \Omega_{\Lambda_1}, i = 1, \dots, r\}, \quad (65)$$

where $\text{vec}(\cdot) : \mathbb{R}^{r \times m} \rightarrow \mathbb{R}^{rm}$ puts the elements of a matrix in a column vector and ϵ is a small positive constant used to have a close set, since typical numerical optimizers only optimize over a close set. Note that $B\Lambda\hat{\theta}_v^T = B\Lambda(\theta_v^T - \theta_v^{*T}) = B\Lambda\theta_v^T - I_r$.

The optimization problem,

$$\begin{aligned} R^2 &= \min_{\theta_v} (\text{vec}(\theta_v - \theta_I^*)^T \text{vec}(\theta_v - \theta_I^*)) \\ \text{s.t.} \quad &\|\text{row}_i(B\Lambda\theta_v^T - I_r)\|^2 = \frac{M_i^2}{M_{\max}^2} - \epsilon, \quad i = 1, \dots, r, \\ &\Lambda \in \Omega_{\Lambda_1}, \\ &\text{vec}(\theta_v) \in \Omega_{\theta}, \end{aligned} \quad (66)$$

which needs to be solved offline, finds the minimum distance, R , from the $\text{vec}(\theta_I^*)$ to the boundary of the set (65). Figure 3 depicts a visualization of the projection boundaries for the case when there are only two adaptive parameters, θ_1 and θ_2 . It is noted that the calculated $\theta_{\max_{i,j}}$ and $\theta_{\min_{i,j}}$ are not unique, and different boundaries can be found by defining different cost functions in (66). After calculating $\theta_{\max_{i,j}}$ and $\theta_{\min_{i,j}}$, the projection parameters region is obtained as,

$$\Omega_{\text{proj}} = \{\text{vec}(\theta_v) : \theta_{i,j} \in [\theta_{\max_{i,j}}, \theta_{\min_{i,j}}]\}. \quad (67)$$

Remark 5. For all elements of Ω_{Λ_1} , the optimization problem (66) finds the largest neighborhood of θ_I^* in Ω_{θ} that satisfies the necessary condition. This neighborhood is an n-sphere, with the center at $\text{vec}(\theta_I^*)$ and with the radius R .

Remark 6. The reason to include $\theta_{I_{i,j}}^*$ inside the projection boundaries is that it is preferred that e converges

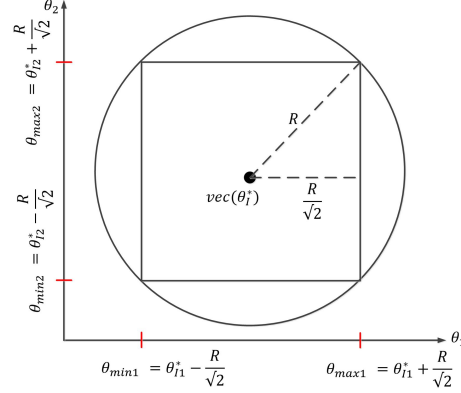


Fig. 3. Projection boundaries when there are two adaptive parameters. The circle defines the border of the neighborhood obtained from the optimization. The square defines the projection boundaries for θ_1 and θ_2 .

to the smallest set around zero. For this, $\theta_{I_{i,j}}^*$ should be inside $[\theta_{\min_{i,j}} + \zeta_{i,j}, \theta_{\max_{i,j}} - \zeta_{i,j}]$ (see (17) and (44)).

In order to show that the optimization problem (66) is feasible, it should be proven that the set E always includes $\text{vec}(\theta_I^*)$.

Theorem 4. The set $\Upsilon = \{\text{vec}(\theta_v) : \|\text{row}_i(B\Lambda\theta_v^T - I_r)\|^2 \leq \frac{M_i^2}{M_{\max}^2} - \epsilon, \Lambda \in \Omega_{\Lambda_1} \subset \Omega_{\Lambda}, i = 1, \dots, r\} \cap \text{vec}(\theta_I^*) \neq \emptyset$ when $\lambda_{\min}(\Lambda) > \gamma \equiv \max_i(1 - \sqrt{\frac{\gamma_{M_i}}{\gamma_{B_i}}})$, where $\lambda_{\min}(\cdot)$ denotes the minimum eigenvalue, $\gamma_{B_i} \equiv \|\text{row}_i(B)\| \|B^T(BB^T)^{-1}\|$ and $\gamma_{M_i} \equiv \frac{M_i^2}{M_{\max}^2} - \epsilon$.

Proof. To prove the non-emptiness of Υ , we should show that $\|\text{row}_i(B\Lambda\theta_I^{*T} - I_r)\|^2 \leq \frac{M_i^2}{M_{\max}^2} - \epsilon$. Using (65) and the definition of $\theta_I^{*T} = B^T(BB^T)^{-1}$, we have,

$$\begin{aligned} &\|\text{row}_i(B\Lambda\theta_I^{*T} - I_r)\|^2 \\ &= \|\text{row}_i(B\Lambda B^T(BB^T)^{-1} - I_r)\|^2 \\ &= \|\text{row}_i(B\Lambda B^T(BB^T)^{-1} - BB^T(BB^T)^{-1})\|^2 \\ &= \|\text{row}_i(B(\Lambda - I_m)B^T(BB^T)^{-1})\|^2 \\ &\leq \|\text{row}_i(B(\Lambda - I_m))\|^2 \|B^T(BB^T)^{-1}\|^2 \\ &\leq (\lambda_{\max}(\Lambda - I_m))^2 \|\text{row}_i(B)\|^2 \|B^T(BB^T)^{-1}\|^2 \\ &= (\lambda_{\min}(\Lambda) - 1)^2 \|\text{row}_i(B)\|^2 \|B^T(BB^T)^{-1}\|^2, \end{aligned} \quad (68)$$

where $\lambda_{\min}(\cdot)$ denotes the minimum eigenvalue. It is noted that since Λ and I_m are diagonal matrices and di-

agonal elements of Λ are between zero and one, we have, $(\lambda_{\max}(\Lambda - I_m))^2 = (\lambda_{\min}(\Lambda) - 1)^2$. Therefore, in order to show that $\|\text{row}_i(B\Lambda\theta_I^{*T} - I_r)\|^2 \leq \frac{M_i^2}{M_{\max}^2} - \epsilon$, for all $i = 1, \dots, r$, we should satisfy

$$\begin{aligned} (\lambda_{\min}(\Lambda) - 1)^2 \|\text{row}_i(B)\|^2 \|B^T(BB^T)^{-1}\|^2 &\leq \frac{M_i^2}{M_{\max}^2} - \epsilon \\ \Rightarrow -\sqrt{\frac{\gamma M_i}{\gamma_{B_i}}} &\leq \lambda_{\min}(\Lambda) - 1 \leq \sqrt{\frac{\gamma M_i}{\gamma_{B_i}}}, \quad i = 1, \dots, r, \end{aligned} \quad (69)$$

where $\gamma_{B_i} \equiv \|\text{row}_i(B)\| \|B^T(BB^T)^{-1}\|$ and $\gamma_{M_i} = \frac{M_i^2}{M_{\max}^2} - \epsilon$ for all $i = 1, \dots, r$. Since the maximum value for the diagonal elements of Λ is one, the only condition that should be satisfied is that $1 - \sqrt{\frac{\gamma_{M_i}}{\gamma_{B_i}}} \leq \lambda_{\min}(\Lambda)$ for $i = 1, \dots, r$ or $\gamma \equiv \max_i(1 - \sqrt{\frac{\gamma_{M_i}}{\gamma_{B_i}}}) \leq \lambda_{\min}(\Lambda)$. \square

Based on the above theorem, and by defining $\gamma_{B_i} \equiv \|\text{row}_i(B)\| \|B^T(BB^T)^{-1}\|$, and $\gamma \equiv \max_i(1 - \frac{M_i}{\gamma_{B_i} M_{\max}})$, the definition of Ω_Λ should be modified as

$$\Omega_{\Lambda_1} = \{\Lambda : \Lambda \in \mathbb{D}^{m \times m}, \text{diag}_i(\Lambda) \in (\gamma, 1], i = 1, \dots, m\}, \quad (70)$$

where \mathbb{D} denotes the set of real diagonal matrices, and $\text{diag}_i(\cdot) : \mathbb{R}^{m \times m} \rightarrow \mathbb{R}$ provides the i th diagonal element of square matrices.

Remark 7. Using Ω_{Λ_1} , defined in (70), and Ω_{proj} , defined in step 3, the upper bound on $\|\text{row}_i(\Delta B)\| = \|\text{row}_i(B\Lambda\hat{\theta}_v^T)\|$ can be found, which we denote as $\bar{\rho}_i$. Therefore, recalling that M_i is defined as the upper bound on the absolute value of i th virtual control signal v_i , the disturbance \bar{d}_i , which is defined after (8), should be smaller than $M_i - \bar{\rho}_i M_{\max}$, i.e. $\bar{d}_i < M_i - \bar{\rho}_i M_{\max}$. Note that $\bar{\rho}_i < \frac{M_i}{M_{\max}}$ is guaranteed by the solution of (66). Therefore, the condition $|d_i| < M_i$ is satisfied.

5 Controller design

In this section, a design procedure for the controller that generates the virtual control signal v in (63) is proposed.

During the design of the controller, the following two assumptions are made about the plant dynamics:

Assumption 1. The dynamics in (63) can be written as

$$\begin{bmatrix} \dot{x}^{(1)} \\ \dot{x}^{(2)} \end{bmatrix} = \begin{bmatrix} A_{1,1} & A_{1,2} \\ A_{2,1} & A_{2,2} \end{bmatrix} \begin{bmatrix} x^{(1)} \\ x^{(2)} \end{bmatrix} + B_v(v+d), \quad y = C \begin{bmatrix} x^{(1)} \\ x^{(2)} \end{bmatrix}, \quad (71)$$

where $A_{1,1} \in \mathbb{R}^{(n-r) \times (n-r)}$ is a Hurwitz matrix, $A_{1,2} \in \mathbb{R}^{(n-r) \times r}$, $A_{2,1} \in \mathbb{R}^{r \times (n-r)}$, $A_{2,2} \in \mathbb{R}^{r \times r}$, $x^{(1)} \in \mathbb{R}^{(n-r)}$, $x^{(2)} \in \mathbb{R}^r$, $y \in \mathbb{R}^r$ and $C = [0_{r \times (n-r)} \quad I_r]$.

Assumption 2. The matrix $B_v \in \mathbb{R}^{n \times r}$ is in the form $[0_{r \times (n-r)} \quad I_r]^T$.

Both of the above assumptions are justified for typical aircraft models [16, 40]. In the simulation section, these assumptions are validated using the AeroData Model in Research Environment (ADMIRE) [25, 50].

Remark 8. For systems for which Assumption 2 does not hold, given that B_v has full column rank, it is possible to find (see [3, 12]) a transformation matrix, T_B , such that $\hat{B}_v = T_B B_v = [0_{r \times (n-r)} \quad I_r]^T$. However, employing this transformation may lead to a state space realization which violates Assumption 1.

Remark 9. It is desired to design a controller which makes $y = Cx = x^{(2)}$ follow the reference input. Since $A_{1,1}$ is Hurwitz, by Assumption 1, showing that the states $x^{(2)}$ are bounded will be sufficient to demonstrate for the boundedness of $x^{(1)}$.

5.1 Dynamics on the Time Varying Sliding Surface

The sliding surface, inspired by [12], is given as

$$\begin{aligned} s(x^{(2)}(t), x^{(2)}(t_0), t) = \\ x^{(2)}(t) - x^{(2)}(t_0)e^{-\bar{\lambda}(t-t_0)} - \frac{2}{\pi}r(t)\tan^{-1}(\bar{\lambda}(t-t_0)) = 0, \end{aligned} \quad (72)$$

where $\bar{\lambda} > 0$ is a scalar parameter, $x^{(2)} \in \mathbb{R}^r$ is defined in (71), $s \in \mathbb{R}^r$ is the sliding surface, and $r(t) \in \mathbb{R}^r$ is the reference to be tracked.

The response of a system controlled by a sliding mode controller includes two phases. The first phase is called the reaching phase. During this phase, the controller

drives the system towards the sliding surface so that $s(t) \rightarrow 0$. In the second, sliding phase, the trajectory evolves on the sliding manifold. For the sliding surface (72), no reaching phase exists since the sliding surface is a function of the initial condition and the trajectories are on the sliding surface at $t = t_0$ i.e. $s(x^{(2)}(t), x^{(2)}(t_0), t_0) = 0$. In the next subsection, via Theorem 5, the control law v that ensures that the trajectories remain on the sliding surface for all $t \geq t_0$ is provided.

Using (72), the trajectories of $x^{(2)}$ on the sliding surface satisfy

$$x^{(2)}(t) = x^{(2)}(t_0)e^{-\bar{\lambda}(t-t_0)} + \frac{2}{\pi}r(t)\tan^{-1}(\bar{\lambda}(t-t_0)). \quad (73)$$

For A satisfying Assumption 1, and if (73) holds, it follows that

$$\begin{aligned} \dot{x}^{(1)} &= A_{1,1}x^{(1)} + A_{1,2}[x^{(2)}(t_0)e^{-\bar{\lambda}(t-t_0)} \\ &\quad + \frac{2}{\pi}r(t)\tan^{-1}(\bar{\lambda}(t-t_0))]. \end{aligned} \quad (74)$$

By defining $G_1 \equiv A_{1,2}x^{(2)}(t_0)$, and $G_2(t) = \frac{2}{\pi}A_{1,2}r(t)\tan^{-1}(\bar{\lambda}(t-t_0))$, we have,

$$\dot{x}^{(1)} = A_{1,1}x^{(1)} + G_1e^{-\bar{\lambda}(t-t_0)} + G_2(t) = A_{1,1}x^{(1)} + g(t), \quad (75)$$

where $g(t) \equiv G_1e^{-\bar{\lambda}(t-t_0)} + G_2(t)$.

Lemma 4. When $x^{(2)}(t)$ is on the sliding surface (72), $x^{(1)}(t)$ and $x^{(2)}(t)$ are bounded and for all $t \geq t_0$, $\|x^{(1)}(t)\| \leq k\bar{x}^{(1)}(t_0) + K_2\bar{x}^{(2)}(t_0) + K_2\bar{r}$, where $K_2 = \frac{k}{\xi}\|A_{1,2}\|$, and where k and ξ are constants. Also, $\bar{x}^{(1)}(t_0)$, $\bar{x}^{(2)}(t_0)$ and \bar{r} are the upper bounds of $\|x^{(1)}(t_0)\|$, $\|x^{(2)}(t_0)\|$ and $\sup_{t \geq t_0} \|r(t)\|$, respectively. Furthermore, $\lim_{t \rightarrow \infty} y(t) = r(t)$.

Proof. Per Assumption 1, $A_{1,1}$ is Hurwitz, hence the homogeneous system $\dot{x}_h^{(1)}(t) = A_{1,1}x_h^{(1)}(t)$ is globally exponentially stable at the origin. The solution of this system is given as $x_h^{(1)}(t) = \Phi(t, t_0)x_h^{(1)}(t_0)$, where $\Phi(t, t_0)$ is the state transition matrix and there exist constants $k > 0$ and $\xi > 0$ such that

$$\|\Phi(t, t_0)\| \leq ke^{-\xi(t-t_0)}, \quad \forall t \geq t_0. \quad (76)$$

Since the state transition matrices of $\dot{x}_h^{(1)}(t) = A_{1,1}x_h^{(1)}(t)$ and $\dot{x}^{(1)}(t) = A_{1,1}x^{(1)}(t) + g(t)$ are the same, we use the state transition matrix $\Phi(t, t_0)$ used in (76) to provide the solution of (75) as

$$x^{(1)}(t) = \Phi(t, t_0)x^{(1)}(t_0) + \int_{t_0}^t \Phi(t, \eta)g(\eta)d\eta. \quad (77)$$

Taking the norm of both sides of (77), we obtain that

$$\|x^{(1)}(t)\| \leq \|\Phi(t, t_0)x^{(1)}(t_0)\| + \int_{t_0}^t \|\Phi(t, \eta)\| \|g(\eta)\| d\eta. \quad (78)$$

Using the definition of $g(t)$ given after (75), it follows that $\|g(t)\| = \|G_1e^{-\bar{\lambda}t} + G_2(t)\| \leq \|G_1\| + \sup_{t \geq t_0} \|G_2(t)\|$. Note that $G_2(t)$ is a function of the reference input $r(t)$, and that $\sup_{t \geq t_0} \|G_2(t)\|$ exists. Therefore, $\|g(t)\| \leq \|A_{1,2}\| \|x^{(2)}(t_0)\| + \|A_{1,2}\| \|r(t)\|$. Defining $K_1 = \|A_{1,2}\| \|x^{(2)}(t_0)\| + \|A_{1,2}\| \bar{r}$, where \bar{r} is the upper bound on $\|r(t)\|$ for $t \geq 0$, and using (76), (78) can be written as,

$$\begin{aligned} \|x^{(1)}(t)\| &\leq k\|x^{(1)}(t_0)\|e^{-\xi(t-t_0)} + kK_1 \int_{t_0}^t e^{-\xi(t-\eta)} d\eta \\ &\leq k\|x^{(1)}(t_0)\|e^{-\xi(t-t_0)} + kK_1 \frac{1}{\xi}(1 - e^{-\xi(t-t_0)}) \\ &\leq k\|x^{(1)}(t_0)\| + kK_1 \frac{1}{\xi} \\ &\leq k\bar{x}^{(1)}(t_0) + K_2\bar{x}^{(2)}(t_0) + K_2\bar{r}, \end{aligned} \quad (79)$$

where $K_2 = \frac{k}{\xi}\|A_{1,2}\|$, while $\bar{x}^{(1)}(t_0)$ and $\bar{x}^{(2)}(t_0)$ represent bounds on $\|x^{(1)}(t_0)\|$ and $\|x^{(2)}(t_0)\|$, respectively. Since the reference signal $r(t)$, $x^{(1)}(t_0)$ and $x^{(2)}(t_0)$ are bounded, (79) shows that $x^{(1)}(t)$ is bounded. Since $x(t_0)$ and $r(t)$ are bounded, it can be shown, using (73), that $x^{(2)}(t)$ is bounded and converges to $r(t)$. Since $y = x^{(2)}$, this completes the proof. \square

5.2 Control Law

We now describe the control law and characterize its properties.

Definition 1. $\text{sign}_v(a)$, where a is a column vector, is a diagonal matrix whose elements are the signs of the

elements of the vector a . For example, $\text{sign}_v([a_1 \ a_2]^T) = \text{diag}(\text{sign}(a_1), \text{sign}(a_2))$, where a_1 and a_2 are scalars.

Definition 2. $|a|_v \equiv \text{sign}_v(a)a$ and $|a^T|_v \equiv a^T \text{sign}_v(a)$, where a is a column vector and $\text{sign}_v(\cdot)$ is defined in Definition 3. For example, $[[a_1 \ a_2]]_v = [a_1 \ a_2] \text{sign}_v([a_1 \ a_2]^T) = [[a_1| \ |a_2|]]$, where a_1 and a_2 are scalars.

Theorem 5. Consider the dynamics in (71), with disturbance d , $t_0 = 0$, and the control law,

$$\begin{aligned} v(t) = & -A_{2,1}x^{(1)}(t) - A_{2,2}x^{(2)}(t) - \bar{\lambda}x^{(2)}(0)e^{-\bar{\lambda}t} \\ & + \frac{2}{\pi}\dot{r}(t)\tan^{-1}(\bar{\lambda}t) + \frac{2}{\pi}r(t)\frac{\bar{\lambda}}{1 + \bar{\lambda}^2t^2} \\ & - \text{sign}_v(s(x^{(2)}(t), x^{(2)}(0), t))\rho, \end{aligned} \quad (80)$$

where $\rho \in R^r$ contains the upper bounds on the absolute values of the elements of the disturbance vector d , and $s(x^{(2)}(t), x^{(2)}(0), t)$ is the sliding surface (72). Then the trajectories of $x^{(2)}$ stay on the sliding surface (72).

Proof. Consider a Lyapunov function candidate $V_2(s) = \frac{1}{2}s^T s$, where the arguments of $s(x^{(2)}(t), x^{(2)}(t_0), t)$ are dropped for clarity. By taking the derivative of V_2 , and using (72) with $t_0 = 0$, we obtain,

$$\begin{aligned} \dot{V}_2 = s^T \dot{s} = & s^T \left(\dot{x}^{(2)}(t) + \bar{\lambda}x^{(2)}(0)e^{-\bar{\lambda}t} - \frac{2}{\pi}\dot{r}(t)\tan^{-1}(\bar{\lambda}t) \right. \\ & \left. - \frac{2}{\pi}r(t)\frac{\bar{\lambda}}{1 + \bar{\lambda}^2t^2} \right). \end{aligned} \quad (81)$$

Using (71) and Assumption 2, we have $\dot{x}^{(2)}(t) = A_{2,1}x^{(1)}(t) + A_{2,2}x^{(2)}(t) + v + d$. By substituting it in (81) we have

$$\begin{aligned} \dot{V}_2 = s^T \dot{s} = & s^T \left(A_{2,1}x^{(1)}(t) + A_{2,2}x^{(2)}(t) + v + d \right. \\ & \left. + \bar{\lambda}x^{(2)}(0)e^{-\bar{\lambda}t} - \frac{2}{\pi}\dot{r}(t)\tan^{-1}(\bar{\lambda}t) - \frac{2}{\pi}r(t)\frac{\bar{\lambda}}{1 + \bar{\lambda}^2t^2} \right). \end{aligned} \quad (82)$$

By substituting the control law (80) into (82), and using Definitions 1 and 2, it follows that

$$\begin{aligned} \dot{V}_2 = s^T [d - \text{sign}_v(s)\rho] = & s^T d - |s^T|_v \rho \\ \leq & |s^T|_v (|d|_v - \rho). \end{aligned} \quad (83)$$

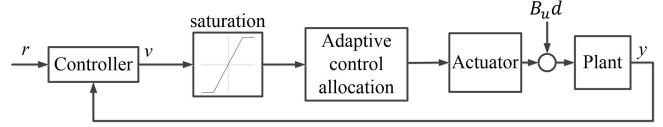


Fig. 4. Block diagram of the closed loop system with soft saturation.

Since ρ contains the upper bounds on the absolute values of the elements of the disturbance vector d , the elements of $|d|_v - \rho$ are non-positive, which leads to $\dot{V}_2 \leq 0$, and consequently proves that $x^{(2)}$ trajectories which are on sliding surface at $t = t_0$, will remain there for all $t > 0$. \square

5.3 Bounding the control input

Remark 10. Up until now, we showed that the control signal v given in (80) keeps $x^{(2)}$ trajectories on the sliding surface defined in (72), and as long as the states of the system remain on the sliding surface, the system output y follows the reference r while all the states remain bounded. In the control allocation development, we stated that the boundedness of the control signal v is ensured by using a soft saturation bound, the limits of which are set in Section 4 as $v_i \in [-M_i, M_i]$, $i = 1, \dots, r$. The overall closed loop system block diagram is presented in Figure 4. In this section, we provide a method inspired by [12], to make sure that the control signal v remains within this saturation bounds.

To ensure that $|v_i| \leq M_i$ for $i = 1, \dots, r$, the following inequality, obtained by using (80), should be satisfied for all $i = 1, \dots, r$,

$$\begin{aligned} |v_i(t)| = & \left| - \sum_{j=1}^n a_{2,i,j} x_j(t) - \bar{\lambda}x_{n-r+i}(0)e^{-\bar{\lambda}t} \right. \\ & \left. + \frac{2}{\pi}\dot{r}_i(t)\tan^{-1}(\bar{\lambda}t) + \frac{2}{\pi}r_i(t)\frac{\bar{\lambda}}{1 + \bar{\lambda}^2t^2} \right. \\ & \left. - \bar{s}_i(x(t))\rho_i \right| \leq M_i, \end{aligned} \quad (84)$$

where x_j , r_i , \dot{r}_i and ρ_i denote the j th component of $x(t)$ and i th components of $r(t)$, $\dot{r}(t)$ and ρ , respectively. Moreover, $\bar{s}_i(x(t))$ is the i th diagonal element of $\text{sign}_v(s(x^{(2)}(t), x^{(2)}(0), t))$. Defining $A_1 = [A_{1,1} \ A_{1,2}]$, $A_2 = [A_{2,1} \ A_{2,2}]$, where $A_{i,j}$ is defined in (74), $a_{2,i,j}$ refer to the elements of A_2 . Using the inequalities $|a - b| < |a| + |b|$ and $|a + b| < |a| + |b|$ for two scalars a and b ,

it can be shown that satisfying the following inequality, ensures (84):

$$\left| \sum_{j=1}^n a_{2i,j} x_j \right| + \left| \bar{\lambda} x_{n-r+i}(0) e^{-\bar{\lambda} t} \right| + \left| \frac{2}{\pi} \dot{r}_i \tan^{-1}(\bar{\lambda} t) \right| + \left| \frac{2}{\pi} r_i \frac{\bar{\lambda}}{1 + \bar{\lambda}^2 t^2} \right| \leq (M_i - \rho_i). \quad (85)$$

Remembering that ρ_i is the upper bound of the disturbance element d_i , and $|d_i|$ is always smaller than M_i (see Remark 4), we obtain that $(M_i - \rho_i) > 0$, meaning that the right hand side of the inequality (85) is positive.

It can then be shown that satisfying the following inequality ensures (85)

$$\left(\left| \sum_{j=1}^n a_{2i,j} x_j \right| + \left| \dot{r}_i \right| - M_i + \rho_i \right) + \bar{\lambda} \left(\left| x_{n-r+i}(0) \right| + \frac{2}{\pi} \left| r_i \right| \right) \leq 0. \quad (86)$$

Remembering that $x^{(1)} = [x_1, \dots, x_{n-r}]^T$ and $x^{(2)} = [x_{n-r+1}, \dots, x_n]^T$, and using (73), it follows that $|x_{n-r+i}(t)| \leq |x_{n-r+i}(0)| + |r_i(t)|$ for $i = 1, \dots, r$, and $\|x^{(1)}(t)\| \geq x_j$ for all $j = 1, \dots, n-r$.

$$\left(\left| \sum_{j=1}^{n-r} a_{2i,j} x_j \right| + \left| \sum_{j=n-r+1}^n a_{2i,j} (|x_{n-r+i}(0)| + |r_i|) \right| + \left| \dot{r}_i \right| - M_i + \rho_i \right) + \bar{\lambda} \left(\left| x_{n-r+i}(0) \right| + \frac{2}{\pi} \left| r_i \right| \right) \leq 0. \quad (87)$$

Furthermore, the upper bound of $\|x^{(1)}(t)\|$ is obtained in Lemma 4. Therefore, defining $\bar{x}^{(1)}(0)$, $\bar{x}^{(2)}(0)$, \bar{r} , \bar{r}_i and $\bar{\dot{r}}_i$ as bounds on $\|x^{(1)}(0)\|$, $\|x^{(2)}(0)\|$, $\|r(t)\|$, $|r_i(t)|$ and $|\dot{r}_i(t)|$, it can be shown that satisfying the following inequality ensures (86):

$$\left(\left| \sum_{j=1}^{n-r} a_{2i,j} \right| \left(k \bar{x}^{(1)}(0) + (1 + K_2) \bar{x}^{(2)}(0) + K_2 \bar{r} + \bar{r}_i \right) + \bar{\dot{r}}_i - M_i + \rho_i \right) + \bar{\lambda} \left(\left| \bar{x}^{(2)}(0) \right| + \frac{2}{\pi} \left| \bar{r}_i \right| \right) \leq 0, \quad (88)$$

where k and K_2 are defined in Lemma 4. Equation (88)

can be rewritten as

$$W_{i,1} + \bar{\lambda} W_{i,2} \leq 0, \quad (89)$$

where $W_{i,1}$ is the first term, and $W_{i,2}$ is the term multiplying $\bar{\lambda}$ in (88). Note that $W_{i,1}$ and $W_{i,2}$ are functions of $\bar{x}^{(1)}(0)$, $\bar{x}^{(2)}(0)$, \bar{r}_i , and $\bar{\dot{r}}_i$ and remain constant along the closed-loop trajectory. Since $W_{i,2}$ is positive, a value of $\bar{\lambda} > 0$ satisfying (89) can always be found if $W_{i,1} < 0$, which can be realized by putting suitable bounds on $\bar{x}^{(1)}(0)$, $\bar{x}^{(2)}(0)$, \bar{r} , \bar{r}_i and $\bar{\dot{r}}_i$. A step by step design procedure to determine the controller parameters is given in the Appendix.

6 SIMULATION RESULTS

The Aerodata Model in Research Environment (ADMIRE), which represents the dynamics of an over-actuated aircraft model, is used to demonstrate the effectiveness of the adaptive control allocation in the presence of uncertainty. The linearized ADMIRE model is introduced in [25], and is given below:

$$\begin{aligned} x &= [\alpha \ \beta \ p \ q \ r]^T \\ y &= [p \ q \ r]^T \\ u &= [u_c \ u_{re} \ u_{le} \ u_r]^T \\ \dot{x} &= Ax + B_u u = Ax + B_v v \\ v &= Bu, \quad B_u = B_v B, \quad B_v = \begin{bmatrix} 0_{2 \times 3} \\ I_{3 \times 3} \end{bmatrix}, \end{aligned} \quad (90)$$

where α, β, p, q and r are the angle of attack, sideslip angle, roll rate, pitch rate and yaw rate, respectively. u represents the control surface deflections vector which consists of canard wings, right and left elevons and the rudder. The state and control matrices are given by:

$$A = \begin{bmatrix} -0.5432 & 0.0137 & 0 & 0.9778 & 0 \\ 0 & -0.1179 & 0.2215 & 0 & -0.9661 \\ 0 & -10.5123 & -0.9967 & 0 & 0.6176 \\ 2.6221 & -0.0030 & 0 & -0.5057 & 0 \\ 0 & 0.7075 & -0.0939 & 0 & -0.2127 \end{bmatrix}, \quad (91)$$

$$B_u = \begin{bmatrix} 0.0069 & -0.0866 & -0.0866 & 0.0004 \\ 0 & 0.0119 & -0.0119 & 0.0287 \\ 0 & -4.2423 & 4.2423 & 1.4871 \\ 1.6532 & -1.2735 & -1.2735 & 0.0024 \\ 0 & -0.2805 & 0.2805 & -0.8823 \end{bmatrix}. \quad (92)$$

The position limits of the control surfaces are given as

$$u_c \in [-55, 25] \times \frac{\pi}{180} rad, \quad u_{re}, u_{le}, u_r \in [-30, 30] \times \frac{\pi}{180} rad,$$

with first-order dynamics and a time constant of 0.05(sec). Note that the control surfaces influence on derivatives of the first two states i.e. $\dot{\alpha}$ and $\dot{\beta}$ is neglected, that is the control surfaces are considered to be pure moment generators, so that control allocation implementation becomes possible [25].

To represent actuator loss of effectiveness and disturbance, a diagonal matrix Λ and a vector d_u , respectively, are augmented to the model (90) as

$$\begin{aligned} \dot{x} &= Ax + B_u \Lambda u + B_u d_u = Ax + B_v v + B_v \bar{d} \\ v &= B \Lambda u, \quad \bar{d} = B d_u, \quad B_u = B_v B, \quad B_v = \begin{bmatrix} 0_{2 \times 3} \\ I_{3 \times 3} \end{bmatrix}. \end{aligned} \quad (93)$$

The system (93) with state and input matrices (92) can be decomposed into two subsystems:

$$\begin{aligned} \begin{bmatrix} \dot{\alpha} \\ \dot{\beta} \end{bmatrix} &= \begin{bmatrix} -0.5432 & 0.0137 \\ 0 & -0.1179 \end{bmatrix} \begin{bmatrix} \alpha \\ \beta \end{bmatrix} \\ &+ \begin{bmatrix} 0 & 0.9778 & 0 \\ 0.2215 & 0 & -0.9661 \end{bmatrix} \begin{bmatrix} p \\ q \\ r \end{bmatrix}, \\ \begin{bmatrix} \dot{p} \\ \dot{q} \\ \dot{r} \end{bmatrix} &= \begin{bmatrix} 0 & -10.5123 \\ 2.6221 & -0.0030 \\ 0 & 0.7075 \end{bmatrix} \begin{bmatrix} \alpha \\ \beta \end{bmatrix} \\ &+ \begin{bmatrix} -0.9967 & 0 & 0.6176 \\ 0 & -0.5057 & 0 \\ -0.0939 & 0 & -0.2127 \end{bmatrix} \begin{bmatrix} p \\ q \\ r \end{bmatrix} + v + \bar{d}. \end{aligned}$$

These two subsystem representation satisfy the assumptions required for implementing the sliding mode controller design in the previous section. In the simulations, the disturbance \bar{d} is a sinusoidal function with amplitude 0.1 and frequency 1 rad/s while a zero-mean white Gaussian noise with standard deviation $\sigma_x = 0.0035$ rad represents the measurement noise. Following the steps in the Appendix, the controller design parameter $\bar{\lambda}$ is calculated as $\bar{\lambda} = 3$. In addition, to avoid chattering, a boundary layer approach is implemented [9].

The simulation results for a conventional pseudo inverse based control allocation are reported in Figure 5 for the case without actuator loss of effectiveness, that is, $\Lambda_1 = I$.

With the actuator loss of effectiveness modeled as

$$\Lambda_2(t) = \begin{cases} \text{diag}(1, 1, 1, 1) & \text{for } t < 7(\text{sec}), \\ \text{diag}(0.85, 0.85, 0.85, 0.85) & \text{for } t \geq 7(\text{sec}), \end{cases}$$

the simulation results for the conventional control allocation are given in Figure 6. It is seen that 15% loss of effectiveness in all actuators at $t = 7$ sec causes instability.

The proposed adaptive control allocation introduced in Section III will be used in the following simulations. Using Steps 1-3 in Section IV, the values of $M_1 = 1.4$, $M_2 = 1.4$ and $M_3 = 0.3$ are obtained and Ω_{proj} , which determines the maximum and minimum of each element of the adaptive parameter matrix is computed corresponding to $\theta_{v_{1,1}} \in [-0.0129, 0.0129]$, $\theta_{v_{1,2}} \in [0.0307, 0.5225]$, $\theta_{v_{1,3}} \in [-0.1357, 0.1371]$, $\theta_{v_{1,4}} \in [-0.212, 0]$, $\theta_{v_{2,1}} \in [-0.3149, -0.1113]$, $\theta_{v_{2,2}} \in [-0.217, -0.1416]$, $\theta_{v_{2,3}} \in [-0.0241, 0.2363]$, $\theta_{v_{2,4}} \in [-0.4162, -0.01]$, $\theta_{v_{3,1}} \in [0.1587, 0.1977]$, $\theta_{v_{3,2}} \in [0.0673, 0.0675]$, $\theta_{v_{3,3}} \in [-0.001, 0.001]$, $\theta_{v_{3,4}} \in [-1.2755, -0.7641]$. We use a closed loop reference model with $l = 4$ and A_m selected as

$$A_m = - \begin{bmatrix} 0.2 & 0 & 0 \\ 0 & 0.1 & 0 \\ 0 & 0 & 0.1 \end{bmatrix}.$$

Figure 7 shows the simulation results for the system with our adaptive control allocation and the actuator loss of effectiveness matrix $\Lambda_2(t)$.

It is seen that the first two states, α and β , are bounded, and the other states (p , q and r) follow the reference inputs (p_{ref} , q_{ref} and r_{ref}) even after the introduction of 30% actuator loss of effectiveness at $t = 7$ sec. Also, it is seen that the elements of $(B\Lambda u)_i$ for $i = 1, 2, 3$, converge to the virtual control signal elements v_i for $i = 1, 2, 3$. The time histories of the adaptive parameters, which are the elements of θ_v matrix, are shown in Figure 8. Two adaptive parameters are selected to illustrate their deviation inside their projection boundaries in Figure 10.

Another scenario is considered next, where a 50% loss of effectiveness for the control surfaces are simulated, specifically, with

$$\Lambda_3(t) = \begin{cases} \text{diag}(1, 1, 1, 1) & \text{for } t < 7(\text{sec}), \\ \text{diag}(0.5, 0.5, 0.5, 0.5) & \text{for } t \geq 7(\text{sec}). \end{cases}$$

It is seen in Figure 9 that the system remains stable after the introduction of the loss of effectiveness. The time histories of the adaptive parameters, which are the elements of θ_v matrix, are shown in Figure 11. Moreover, two adaptive parameters are selected to illustrate their deviation within their projection boundaries in Figure 12.

7 SUMMARY

An adaptive control allocation for uncertain over-actuated systems with actuator saturation is proposed in this paper. The method needs neither uncertainty identification nor persistence of excitation. A sliding mode controller with time-varying sliding surface is also proposed, to guarantee the stability of the overall closed loop system while realizing reference tracking. The simulation results with the ADMIRE model show the effectiveness of the proposed method.

A Controller design procedure

The following procedure can be followed to obtain the controller design parameters:

Step 1- Use Step 1 in Section IV, to determine M_i , $i = 1, \dots, r$.

Step 2- Calculate Ω_θ using Step 2 in Section IV.

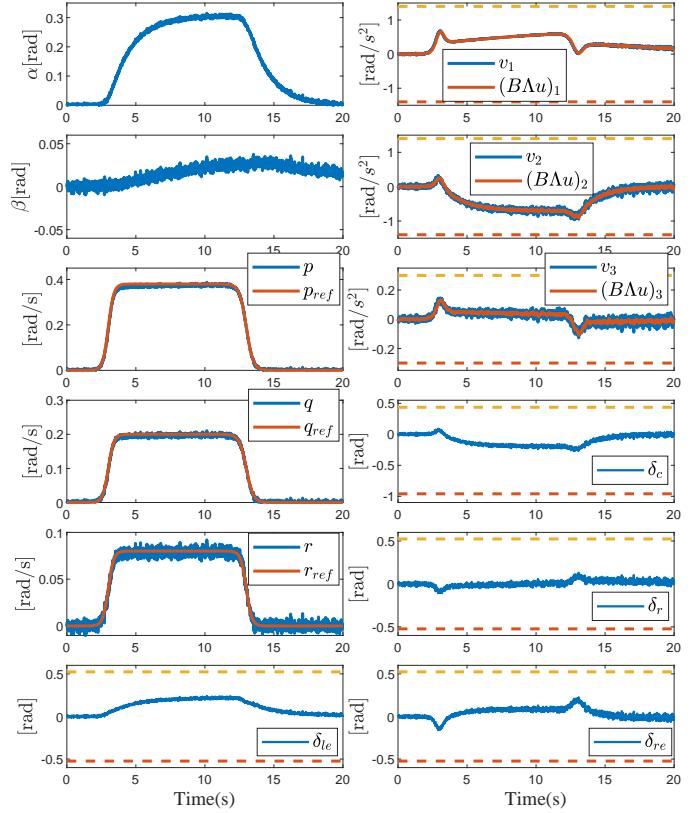


Fig. 5. System states, virtual control signals and actuators' deflections using conventional control allocation when actuator loss of effectiveness is $\Lambda_1 = I$.

Step 3- Using Theorem 4, calculate $\gamma \equiv \max_i(1 - \sqrt{\frac{\gamma_{M_i}}{\gamma_{B_i}}})$, where $M_{\max} = \max_i M_i$, $\gamma_{M_i} \equiv \frac{M_i^2}{M_{\max}^2} - \epsilon$ for a small positive ϵ , and $\gamma_{B_i} \equiv \|\text{row}_i(B)\| \|B^T(BB^T)^{-1}\|$.

Step 4- Using γ , obtain Ω_{Λ_1} in (70).

Step 5- Solve the optimization problem (66), which leads to obtaining the Ω_{proj} , which is defined in Section IV, step 3.

Step 6- Using (70) and Ω_{proj} , calculate $\bar{\rho}_i$ for $i = 1, \dots, r$, which are defined in Remark 4.

Step 9- Calculate k and ξ using (76).

Step 10- In the proposed controller design, since the controllers' goal is reference tracking in the presence of

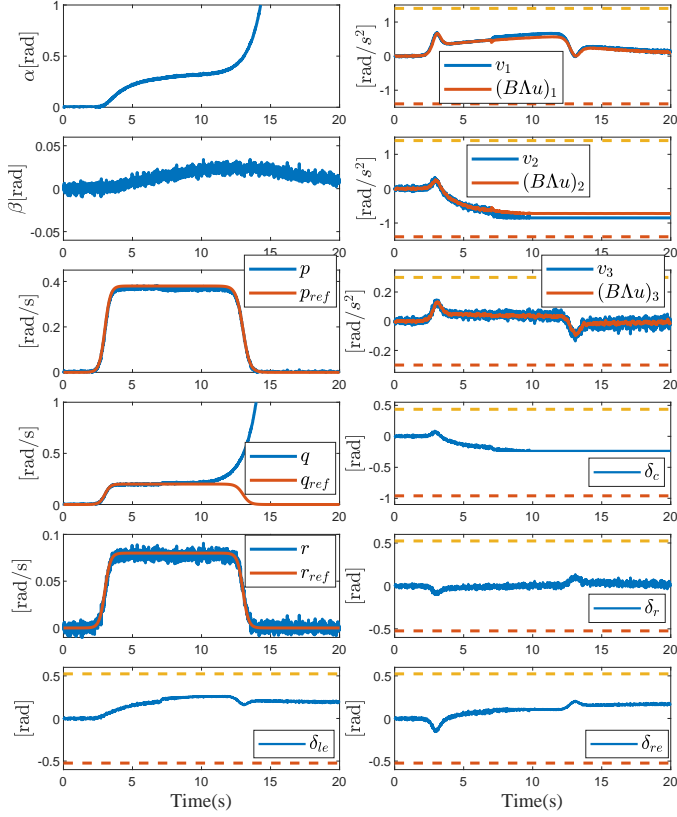


Fig. 6. System states, virtual control signals and actuators' deflections using conventional control allocation when actuator loss of effectiveness is Λ_2 .

saturation, the initial states, $x^{(1)}(0)$ and $x^{(2)}(0)$, the elements of reference input, r , the elements of the derivative of the reference input, \dot{r} , and the elements of disturbance \bar{d} , should be bounded. Let $\bar{x}^{(1)}(0)$, $\bar{x}^{(2)}(0)$, \bar{r}_i , $\bar{\dot{r}}_i$ and \bar{L}_i be upper bounds on the norms of $x^{(1)}(0)$, $x^{(2)}(0)$, r_i , \dot{r}_i and \bar{d}_i , respectively, for $i = 1, \dots, r$. These values can be obtained by an expert, who has information about the plant and its constraints. Also, these values can be written in the data sheets.

Step 11- Check if $W_{i,1} < 0$.

If yes, continue to the next step.

If no, the expert should reduce $\bar{x}^{(1)}(0)$, $\bar{x}^{(2)}(0)$, \bar{r}_i , $\bar{\dot{r}}_i$ and \bar{L}_i to satisfy this inequality. Most of the time, this is done by confining the initial value of states to a smaller

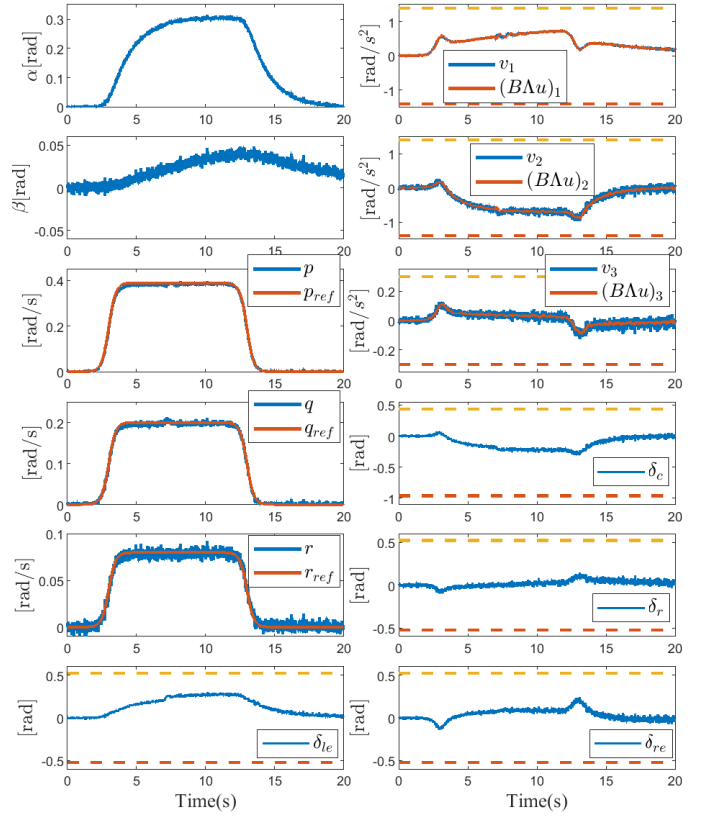


Fig. 7. System states, virtual control signals and actuators' deflections using adaptive control allocation, when actuator loss of effectiveness matrix is Λ_2 .

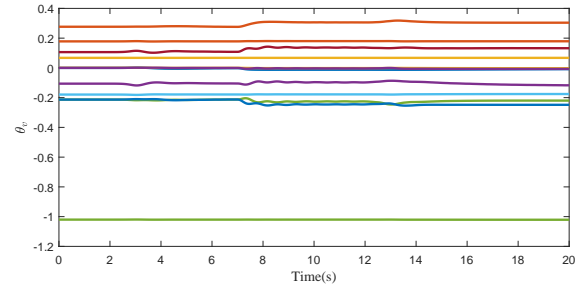


Fig. 8. Adaptive parameters when the actuator loss of effectiveness matrix is Λ_2 .

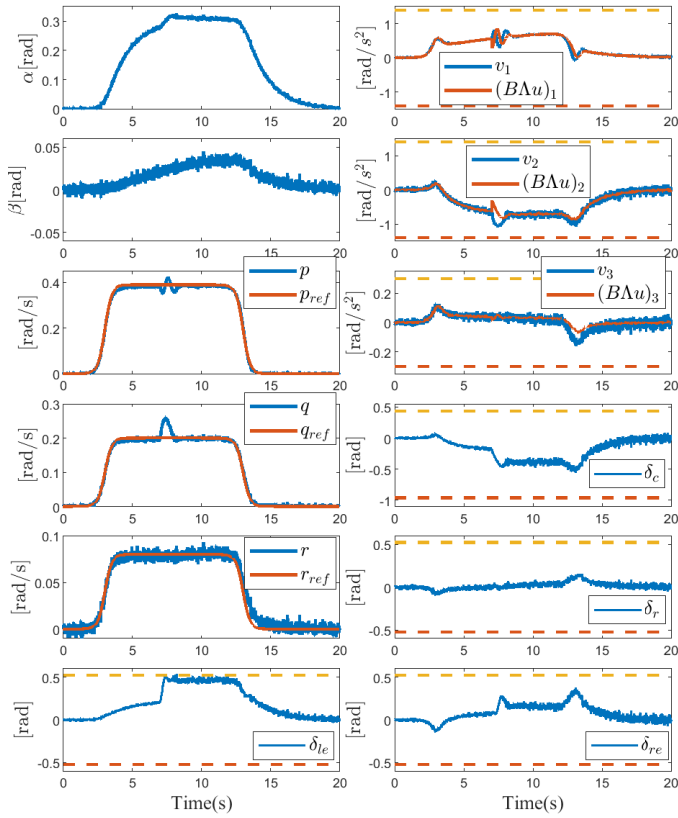


Fig. 9. System states, virtual control signals and actuators' deflections using adaptive control allocation when actuator loss of effectiveness matrix is Λ_3 .

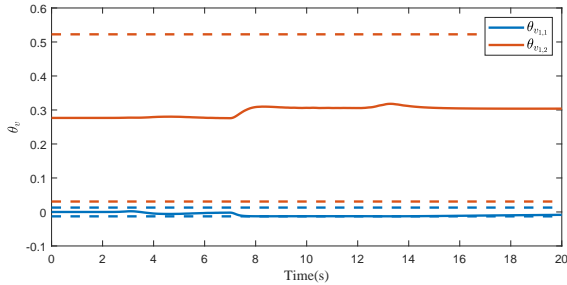


Fig. 10. Two adaptive parameters and their projection boundaries when the actuator loss of effectiveness matrix is Λ_2 . The dashed lines are the projection boundaries.

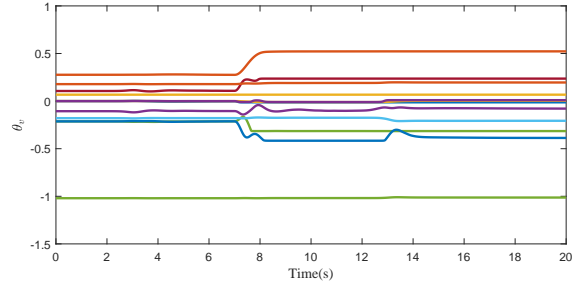


Fig. 11. Adaptive parameters when the actuator loss of effectiveness matrix is Λ_3 .

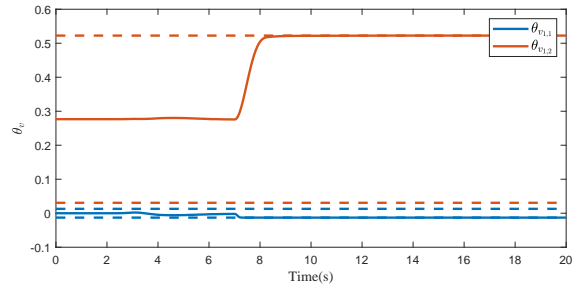


Fig. 12. Two adaptive parameters and their projection boundaries when the actuator loss of effectiveness matrix is Λ_3 . The dashed lines are the projection boundaries.

limit. In this design, it can be done even by reducing the derivative of the reference input, if fast maneuver is not required in the plant.

Step 12- Calculate $W_{i,2}$ in (89).

Step 13- Find a $\bar{\lambda}$ satisfying (89) and design the control signal (80).

References

- [1] Diana M Acosta, Yildiray Yildiz, Robert W Craun, Steven D Beard, Michael W Leonard, Gordon H Hardy, and Michael Weinstein. Piloted evaluation of a control allocation technique to recover from pilot-induced oscillations. *Journal of Aircraft*, 52(1):130–140, 2014.
- [2] Halim Alwi and Christopher Edwards. Fault tolerant control using sliding modes with on-line control allocation. *Automatica*, 44(7):1859–1866, 2008.

- [3] Panos J Antsaklis and Anthony N Michel. *Linear systems*. Springer Science & Business Media, 2006.
- [4] Marc Bodson. Evaluation of optimization methods for control allocation. *Journal of Guidance, Control, and Dynamics*, 25(4):703–711, 2002.
- [5] Kenneth A Bordignon. *Constrained control allocation for systems with redundant control effectors*. PhD thesis, Virginia Tech, 1996.
- [6] Abdelkader Bouarfa, Marc Bodson, and Maurice Fadel. A fast active-balancing method for the 3-phase multilevel flying capacitor inverter derived from control allocation theory. *IFAC-PapersOnLine*, 50(1):2113–2118, 2017.
- [7] James M Buffington and Dale F Enns. Lyapunov stability analysis of daisy chain control allocation. *Journal of Guidance, Control, and Dynamics*, 19(6):1226–1230, 1996.
- [8] Alessandro Casavola and Emanuele Garone. Fault-tolerant adaptive control allocation schemes for overactuated systems. *International Journal of Robust and Nonlinear Control*, 20(17):1958–1980, 2010.
- [9] Min-Shin Chen, Yean-Ren Hwang, and Masayoshi Tomizuka. A state-dependent boundary layer design for sliding mode control. *IEEE transactions on automatic control*, 47(10):1677–1681, 2002.
- [10] Mou Chen, Shuzhi Sam Ge, Bernard Voon Ee How, and Yoo Sang Choo. Robust adaptive position mooring control for marine vessels. *IEEE Transactions on Control Systems Technology*, 21(2):395–409, 2013.
- [11] Maria Letizia Corradini and Andrea Cristofaro. A nonlinear fault-tolerant thruster allocation architecture for underwater remotely operated vehicles. *IFAC-PapersOnLine*, 49(23):285–290, 2016.
- [12] Maria Letizia Corradini, Andrea Cristofaro, and Giuseppe Orlando. Robust stabilization of multi input plants with saturating actuators. *IEEE Transactions on Automatic Control*, 55(2):419–425, 2010.
- [13] Andrea Cristofaro and Tor Arne Johansen. Fault tolerant control allocation using unknown input observers. *Automatica*, 50(7):1891–1897, 2014.
- [14] Andrea Cristofaro, Marios M Polycarpou, and Tor Arne Johansen. Fault diagnosis and fault-tolerant control allocation for a class of nonlinear systems with redundant inputs. In *2015 54th IEEE Conference on Decision and Control (CDC)*, pages 5117–5123. IEEE, 2015.
- [15] Murat Demirci and Metin Gokasan. Adaptive optimal control allocation using lagrangian neural networks for stability control of a 4ws–4wd electric vehicle. *Transactions of the Institute of Measurement and Control*, 35(8):1139–1151, 2013.
- [16] Guillaume JJ Ducard. *Fault-tolerant flight control and guidance systems: Practical methods for small unmanned aerial vehicles*. Springer Science & Business Media, 2009.
- [17] Wayne Durham, Kenneth A. Bordignon, and Roger Beck. *Aircraft Control allocation*. Springer Science & Business Media, 2009.
- [18] Wayne C Durham. Constrained control allocation. *Journal of Guidance, control, and Dynamics*, 16(4):717–725, 1993.
- [19] Christopher Edwards, Thomas Lombaerts, Hafid Smaili, et al. Fault tolerant flight control. *Lecture Notes in Control and Information Sciences*, 399:1–560, 2010.
- [20] Guillermo P Falconí and Florian Holzapfel. Adaptive fault tolerant control allocation for a hexacopter system. In *American Control Conference (ACC), 2016*, pages 6760–6766. IEEE, 2016.
- [21] Sergio Galeani and Mario Sassano. Data-driven dynamic control allocation for uncertain redundant plants. In *2018 IEEE Conference on Decision and Control (CDC)*, pages 5494–5499. IEEE, 2018.
- [22] Travis E Gibson, Zheng Qu, Anuradha M Annaswamy, and Eugene Lavretsky. Adaptive output feedback based on closed-loop reference models. *IEEE Transactions on Automatic Control*, 60(10):2728–2733, 2015.
- [23] Witold Gierusz and Mirosław Tomera. Logic thrust allocation applied to multivariable control of the training ship. *Control Engineering Practice*, 14(5):511–524, 2006.
- [24] Ola Härkegård. Efficient active set algorithms for solving constrained least squares problems in aircraft control allocation. In *Decision and Control, 2002, Proceedings of the 41st IEEE Conference on*, volume 2, pages 1295–1300. IEEE, 2002.
- [25] Ola Härkegård and S Torkel Glad. Resolving actuator redundancyoptimal control vs. control allocation. *Automatica*, 41(1):137–144, 2005.
- [26] Tor A Johansen and Thor I Fossen. Control allocationa survey. *Automatica*, 49(5):1087–1103, 2013.
- [27] Tor A Johansen, Thomas P Fuglseth, Petter Tøndel, and Thor I Fossen. Optimal constrained control allocation in marine surface vessels with rudders. *Control Engineering Practice*, 16(4):457–464, 2008.
- [28] Martin Kirchengast, Martin Steinberger, and Martin Horn. Input matrix factorizations for constrained control allocation. *IEEE Transactions on Automatic Control*, 63(4):1163–1170, 2018.
- [29] Eugene Lavretsky and Travis E Gibson. Projection operator in adaptive systems. *arXiv preprint arXiv:1112.4232*, 2011.
- [30] F Liao, K-Y Lum, JL Wang, and M Benosman. Adaptive control allocation for non-linear systems with internal dynamics. *IET control theory & applications*, 4(6):909–922, 2010.
- [31] John AM Petersen and Marc Bodson. Constrained quadratic programming techniques for control allocation. *IEEE Transactions on Control Systems Technology*, 14(1):91–98, 2006.
- [32] Tarun Kanti Podder and Nilanjan Sarkar. Fault-tolerant control of an autonomous underwater vehicle under thruster redundancy. *Robotics and Autonomous Systems*, 34(1):39–52, 2001.
- [33] M Ehsan Raoufat, Kevin Tomsovic, and Seddik M Djouadi. Dynamic control allocation for damping of inter-

- area oscillations. *IEEE Transactions on Power Systems*, 32(6):4894–4903, 2017.
- [34] Iman Sadeghzadeh, Abbas Chamseddine, Youmin Zhang, and Didier Theilliol. Control allocation and re-allocation for a modified quadrotor helicopter against actuator faults. *IFAC Proceedings Volumes*, 45(20):247–252, 2012.
- [35] Qiang Shen, Danwei Wang, Senqiang Zhu, and Eng Kee Poh. Inertia-free fault-tolerant spacecraft attitude tracking using control allocation. *Automatica*, 62:114–121, 2015.
- [36] Qiang Shen, Danwei Wang, Senqiang Zhu, and Eng Kee Poh. Robust control allocation for spacecraft attitude tracking under actuator faults. *IEEE Transactions on Control Systems Technology*, 25(3):1068–1075, 2017.
- [37] Asgeir J Sørensen. A survey of dynamic positioning control systems. *Annual reviews in control*, 35(1):123–136, 2011.
- [38] Mikkel Eske Nørgaard Sørensen, Søren Hansen, Morten Breivik, and Mogens Blanke. Performance comparison of controllers with fault-dependent control allocation for uavs. *Journal of Intelligent & Robotic Systems*, 87(1):187–207, 2017.
- [39] Johannes Stephan and Walter Fichter. Fast exact redistributed pseudoinverse method for linear actuation systems. *IEEE Transactions on Control Systems Technology*, (99):1–8, 2017.
- [40] Brian L Stevens, Frank L Lewis, and Eric N Johnson. *Aircraft control and simulation: dynamics, controls design, and autonomous systems*. John Wiley & Sons, 2015.
- [41] Hamid D Taghirad and Yousef B Bedoustani. An analytic-iterative redundancy resolution scheme for cable-driven redundant parallel manipulators. *IEEE Transactions on Robotics*, 27(6):1137–1143, 2011.
- [42] Johannes Tjønnås and Tor A Johansen. Adaptive control allocation. *Automatica*, 44(11):2754–2765, 2008.
- [43] Johannes Tjønnås and Tor A Johansen. Stabilization of automotive vehicles using active steering and adaptive brake control allocation. *IEEE Transactions on Control Systems Technology*, 18(3):545–558, 2010.
- [44] Seyed Shahabaldin Tohidi, Ali Khaki Sedigh, and David Buzorgnia. Fault tolerant control design using adaptive control allocation based on the pseudo inverse along the null space. *International Journal of Robust and Nonlinear Control*, 26(16):3541–3557, 2016.
- [45] Seyed Shahabaldin Tohidi, Yildiray Yildiz, and Ilya Kolmanovsky. Fault tolerant control for over-actuated systems: An adaptive correction approach. In *American Control Conference (ACC), 2016*, pages 2530–2535. IEEE, 2016.
- [46] Seyed Shahabaldin Tohidi, Yildiray Yildiz, and Ilya Kolmanovsky. Adaptive control allocation for over-actuated systems with actuator saturation. volume 50, pages 5492–5497. Elsevier, 2017.
- [47] Seyed Shahabaldin Tohidi, Yildiray Yildiz, and Ilya Kolmanovsky. Pilot induced oscillation mitigation for unmanned aircraft systems: An adaptive control allocation approach. In *2018 IEEE Conference on Control Technology and Applications (CCTA)*, pages 343–348. IEEE, 2018.
- [48] John Virnig and David Bodden. Multivariable control allocation and control law conditioning when control effectors limit. In *Guidance, Navigation, and Control Conference*, page 3609, 1994.
- [49] Yildiray Yildiz and Ilya Kolmanovsky. Implementation of capio for composite adaptive control of cross-coupled unstable aircraft. In *Infotech@ Aerospace 2011*, page 1460, 2011.
- [50] Yildiray Yildiz and Ilya Kolmanovsky. Stability properties and cross-coupling performance of the control allocation scheme capio. *Journal of Guidance, Control, and Dynamics*, 34(4):1190–1196, 2011.
- [51] Yildiray Yildiz and Ilya V Kolmanovsky. A control allocation technique to recover from pilot-induced oscillations (capio) due to actuator rate limiting. In *Proceedings of the 2010 American Control Conference*, pages 516–523. IEEE, 2010.
- [52] Yildiray Yildiz, Ilya V Kolmanovsky, and Diana Acosta. A control allocation system for automatic detection and compensation of phase shift due to actuator rate limiting. In *Proceedings of the 2011 American Control Conference*, pages 444–449. IEEE, 2011.
- [53] Luca Zaccarian. Dynamic allocation for input redundant control systems. *Automatica*, 45(6):1431–1438, 2009.
- [54] Youmin Zhang and Jin Jiang. Bibliographical review on reconfigurable fault-tolerant control systems. *Annual reviews in control*, 32(2):229–252, 2008.